#### PREPRINT SUBMITTED

This manuscript is a preprint uploaded to EarthArXiv, not yet peer-reviewed. This preprint was submitted for publication to *Earth Surface Processes and Landforms* in September 2025. Authors encourage downloading the latest manuscript version from EarthArXiv, and welcome comments, feedback and discussions anytime. Please, feel free to get in contact with the first author: gino.de-gelder@univ-grenoble-alpes.fr

# Coral reef and mangrove interplay during Mid- and Late-Holocene sea-level changes in Belitung Island, Indonesia

T. Solihuddin<sup>1\*</sup>, G. de. Gelder<sup>1,2\*</sup>, D. A. Utami<sup>1</sup>, F. Sidik<sup>3</sup>, R. Rachmayani<sup>4</sup>, M. Hendrizan<sup>1</sup>, S. Y. Cahyarini<sup>1</sup>, M. R. Purnama<sup>5</sup>, M. Elliot<sup>6</sup>, L. Husson<sup>2</sup>

<sup>1</sup>Research Center for Climate and Atmosphere, National Research and Innovation Agency, Bandung, Indonesia

<sup>2</sup>ISTerre, IRD, CNRS, University Grenoble Alpes, Grenoble, France

<sup>3</sup>Research Center for Oceanography, National Research and Innovation Agency, Jakarta, Indonesia

<sup>4</sup>Oceanography Research Group, Bandung Institute of Technology, Bandung, Indonesia <sup>5</sup>Macrofossil Belitong, Belitung, Indonesia

<sup>6</sup>Laboratoire de Planétologie et Géodynamique, Université de Nantes, CNRS, France \*authors share first-authorship

Correspondence to: Gino de Gelder (gino.de-gelder@univ-grenoble-alpes.fr)

# Coral reef and mangrove interplay during Mid- and Late-Holocene sea-level changes in Belitung Island, Indonesia

- T. Solihuddin<sup>1\*</sup>, G. de. Gelder<sup>1,2\*</sup>, D. A. Utami<sup>1</sup>, F. Sidik<sup>3</sup>, R. Rachmayani<sup>4</sup>, M. Hendrizan<sup>1</sup>, S. Y. Cahyarini<sup>1</sup>, M. R. Purnama<sup>5</sup>, M. Elliot<sup>6</sup>, L. Husson<sup>2</sup>
- <sup>1</sup>Research Center for Climate and Atmosphere, National Research and Innovation Agency, Bandung, Indonesia
- <sup>2</sup>ISTerre, IRD, CNRS, University Grenoble Alpes, Grenoble, France
- <sup>3</sup>Research Center for Oceanography, National Research and Innovation Agency, Jakarta, Indonesia
- <sup>4</sup>Oceanography Research Group, Bandung Institute of Technology, Bandung, Indonesia
- <sup>5</sup>Macrofossil Belitong, Belitung, Indonesia
- <sup>6</sup>Laboratoire de Planétologie et Géodynamique, Université de Nantes, CNRS, France
- \*authors share first-authorship

#### **Abstract**

Coral reefs and mangrove forests are susceptible coastal ecosystems, particularly in light of intense human-induced pressures, including the anticipated sea-level rise in the 21st century. Here, we explore the chronology and interconnectedness between coral reef and mangrove interplay in response to Holocene sea-level changes, taking Belitung Island, Indonesia, as a case study. We describe the regressive stratigraphy of an outcrop in a drained tin mine and collected a series of 3 m long cores from three study sites, which suggest that the nearshore reef establishment was taking place at ~2 m elevation below the present mean sea level by approximately ~6.1-5.7 kyr BP. After a phase of vertical reef accretion until ca. 4.3-3.8 kyr BP, the reef system—from the forereef to onshore beaches changed to a horizontally prograding system under conditions of relative sea-level fall. The shoreline accordingly prograded seaward, leaving kilometer-wide platforms constructed by the antecedent Mid-Holocene coral reefs, thereby providing accommodation space for terrestrial sediment deposition and mangrove forests that thrived from the Late Holocene onwards. The case study of Belitung Island permits us to derive general behavior laws based on the deterministic role of geological history in the development of coastal ecosystems. By shedding light on the intricate relationship between coral reefs, mangroves, and sea level changes over geological timescales, these results outline the need to analyze the past evolution of these coupled systems to predict their future evolution.

Keywords: Holocene, coral reef, mangrove, sea level, Indonesia

#### Introduction

Coral reefs and mangrove ecosystems are key tropical ecosystems. They grow parallel to tropical coastlines and play important ecological roles in a highly diverse flora and fauna, which are essential to coastal communities (e.g., Guannel et al., 2016; Choudhary et al., 2024). Fossil coral has been shown to document rapid changes in Earth's climate, including sea surface salinity, temperature, light, and turbidity (e.g., Cobb et al., 2013; Falter et al., 2013; Cahyarini et al., 2021; McGregor et al., 2022). In addition, fossil coral reefs document vertical land motion and sea level changes over geological timescales (e.g., Neumann, 1985; Woodroffe, 2002; Collins et al., 2011; Solihuddin et al., 2015; De Gelder et al., 2022, 2023). In this context, it is essential to comprehend reef evolution at geomorphological scales, as it can bridge the temporal and spatial disparity between long-term geological and short-term ecological processes (Buddemeier & Smith, 1988; Woodroffe, 2025). Similar to

coral reefs, mangrove forests provide an important ecological habitat to a wide range of flora and fauna and function as natural carbon sequestration agents in the intertidal zones of subtropical regions (Howard et al., 2017). Mangrove environments provide fish nursery habitats, enhance water quality, and stabilize shorelines to support coral reefs (Wells & Ravilious, 2006; Whitfield, 2017; Rogers & Mumby, 2019). The evolution of mangroves has been closely associated with changes in sea level and climate on geological timescales, with mangroves generally flourishing during temperate periods characterized by relatively high sea levels and humid conditions (Srivastava & Prasad, 2019). Most importantly, coral reefs and mangroves develop an overlooked interconnectedness at ecological, geological, and geomorphological scales. For example, coral reefs dramatically reduce the wave energy coming from offshore, allowing mangroves to grow in a calm wave environment, while mangroves store riverine sediments that could hamper the downstream expansion of coral reefs (Harborne et al., 2006).

Direct observations and remote sensing are convenient and cost-effective ways to track and study coastal changes (Sui et al., 2020; Kamila et al., 2020; Kantamaneni et al., 2022), but current records of coastal dynamics span only a few decades and show relatively minor changes compared to the significant changes anticipated over the next century (Malthus & Mumby, 2003; Vitousek et al., 2023). During the past ~10,000 years (the Holocene), the development of coral reefs and mangroves was largely shaped by changes in relative sea level and environmental factors, including terrigenous inputs and the underlying topography (e.g., Montaggioni, 2005; Woodroffe et al., 2014; Yamano et al., 2019; Woodroffe, 2025). This study focuses on coastal geomorphology and geology, enabling us to go deeper in time and uncover how Holocene variations in sea level on the m-scale have influenced tropical coastlines. To our knowledge, only a few such records are available, with even fewer concentrating on reefs and mangroves as symbiotic, interconnected systems (Yamano et al., 2019; Woodroffe, 2025).

Indonesia is at the heart of the coral reef triangle and also hosts one of the largest mangrove surface areas in the world, which has suffered the most dramatic decline (https:// www.globalmangrovewatch.org/; accessed 15 August 2025). Belitung Island has become a regional benchmarking site, with previous studies focusing on sea-level changes (Suyarso, 2012; Meltzner et al., 2017), mangrove evolution (Yulianto et al., 2019), and geodynamics (Sarr et al., 2019). Furthermore, the coastal area is marked as a geopark heritage site for its unique geological landscape hosting diverse flora and fauna. We aim to characterize how coral reefs and mangroves have evolved on Belitung Island, Indonesia, over the course of the Holocene (past 10,000 years). We utilized a series of sediment cores from three different sites (Sijuk, Petaling, and Batu Itam-Temparan) at the northwestern coast of Belitung Island, where a mangrove forest currently overlies a fossil reef system. These sites represent three different characteristics of mangrove habitat, including sheltered locations with a vast, fluvialdominated environment for Sijuk; exposed shore with an extensive intertidal fringing reef for Batu Itam-Temparan; and island mangroves with narrow fringing reefs for Petaling. The material was radiocarbon dated, which enables dating the vertical and lateral distribution of mangrove forests. The aim of this study is to understand the chronology of the interplay between coral reefs and mangroves on 100-1000-year timescales under the influence of Holocene sea-level change and terrigenous input.

#### Field setting

Belitung Island, Indonesia, is located on the central Sunda Shelf between Sumatra and Borneo and is regionally slowly subsiding, with 0.2–0.3 mm/yr in Belitung (Sarr et al., 2019),

owing to the gradual dynamic tilt of the Sunda Shelf above the subduction zone in the aftermath of the collision of the Australian continent with SE Asia (Husson et al., 2022). Because the Sunda Shelf is extremely shallow, it was permanently continental before MIS11 (around 400 kyr BP) (Sarr et al., 2019). Successive marine transgressions gradually and episodically flooded the shelf, reaching Belitung only during MIS5e (around 125 kyr BP) and the Holocene. This flooding corresponds to the onset of the symbiotic reef/mangrove system in that area, which facilitates the analysis of its past history as well as its present-day and future evolution.

The geology of Sijuk and Batu Itam on the northwest coast of Belitung Island is dominated by the granitic Tanjung Pandan Formation (Fig. 1; 208 to 245 Ma; Priem et al., 1975). Floodplains, river estuaries, and beaches contain alluvial and beach deposits, which primarily consist of gravel, sand, silt, clay, and coral fragments. The geology of Petaling on Mendanau Island, offshore of West Belitung Island, differs from Sijuk and Batu Itam. It consists of metasandstone that alternates with slate, mudstone, shale, tuffaceous siltstone, and chert from the Kelapakampit Formation (Fig. 1). The fossil assemblage indicates their Permo-Carboniferous age. Gravel, sand, silt, and clay primarily constitute the alluvial and beach deposits found in the river estuaries and beaches.

Belitung Island is located in the Karimata Strait, off the east coast of Sumatra, Indonesia, which directly borders the South China Sea to the north (Fig. 1). The island has a tropical climate that is significantly influenced by the seasonally reversing surface currents of the Karimata Strait and coupled monsoonal winds (Xu et al., 2021). Because the patterns of oceanic circulation are highly dependent on the bathymetry of the shelf, the current regime is extremely dynamic (Susilohadi et al., 2024). During the boreal winter monsoon (from November to March), southward oceanic currents from the South China Sea bring wetter climatic conditions and low-salinity waters. Conversely, during the boreal summer monsoon (from May to September), the current reverses and the surface waters flow westward, driving drier conditions to the region (Wyrtki, 1961; Susanto et al., 2001). The significant wave height on Belitung Island is estimated to be between 0.1 and 0.5 m, with greater values during the west monsoon (Pamungkas, 2018). The normal tide is semi-diurnal, with a tidal range of up to 2.5–3 m on a spring tide (Pamungkas, 2018). The ocean temperatures in the Bangka Belitung Islands region range from 28 to 30°C. According to BATNAS bathymetry, from the Geospatial Information Agency of Indonesia (BIG, 2024) through https://tanahair.indonesia.go.id/demnas/#/batnas, the bathymetry of the region is predominantly shallow, seldom surpassing a depth of 60 m (Fig. 1). These geomorphic, oceanographic, and climate settings have a significant impact on the coral reef and mangrove habitats in the region.

# Holocene sea level reconstructions at Belitung Island

Belitung Island is located in the far-field, where horizontal tectonic deformation is nonexistent and glacio-isostatic adjustment (GIA) is relatively small (Tjia & Liew, 1996; Mann et al., 2019; Li et al., 2023). Several studies constrain Holocene relative sea-level variations on Belitung Island and surrounding areas (Fig. 2; Geyh et al., 1979; Tjia, 1996; Hesp et al., 1998; Suyarso, 2012; Meltzner et al., 2017; Sarr et al., 2019; Yulianto et al., 2019). Geyh et al. (1979), Tjia (1996), and Hesp et al. (1998) described the peak Holocene sea-level highstand at about +5.8 m, +4 m, and +3 m above present mean sea level (PMSL) on the Malacca Strait, Malay-Thai Peninsula, and Singapore, respectively, and its gradual fall to current levels thereafter in the mid-to-late Holocene. Suyarso (2012) found three separate *Ostrea sp.* fossil sites on Belitung Island. These revealed two transgressions and one regression,

with sea levels 2.5 m and 2.0 m above PMSL, respectively, between 5 and 2.6 kyr BP. Microatoll dating suggests a 1.5-meter-high above PMSL mid-Holocene highstand at Belitung around 6.5 kyr BP (Meltzner et al., 2017). Recent regional compilations suggest Sunda Shelf Mid-Holocene sea-level peaks of  $\sim$ 0–7 m above the PMSL (Mann et al., 2019; Li et al., 2023), with GIA predictions for Belitung Island around  $\sim$ 3 ± 3 m (Li et al., 2023).

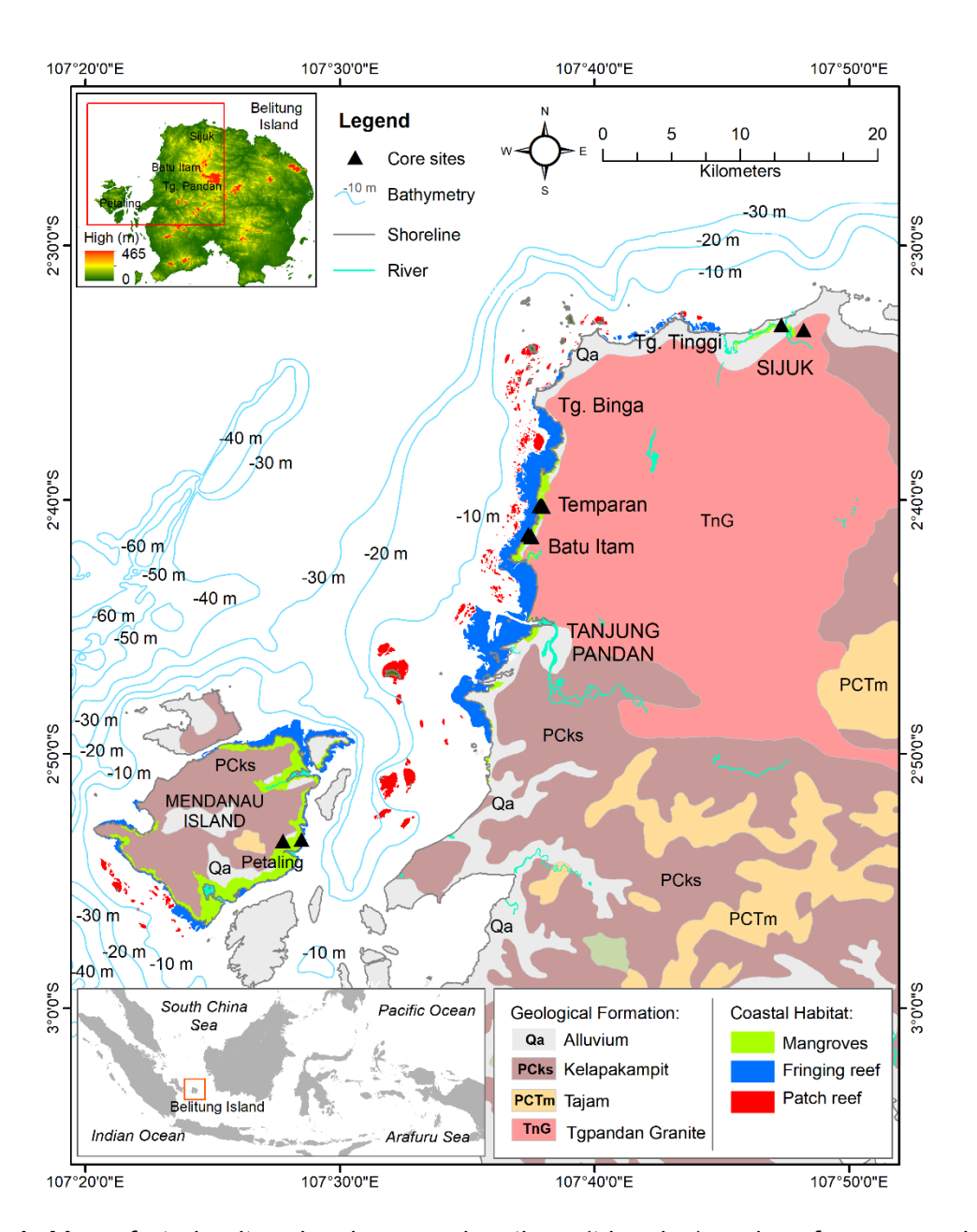


**Figure 1.** Map of study site, showing core locations (triangles) and reef-mangrove habitat distribution. Basemap is regional geology (after Baharuddin & Sidarto, 1995). Bathymetry from the Geospatial Information Agency of Indonesia (BIG, 2024). Reef and mangrove habitats, as of 2021, were mapped from WorldView-2 image, at a resolution of 0.6 m, and ground-truthed in 2022 and 2023.

Sarr et al. (2019) proposed that Belitung Island is currently subsiding at a rate of 0.2–0.3 mm/yr, based on a combination of numerical modeling of reef growth, morphological observations, and radiocarbon dating from corals buried 3 km inland that attest to seaward

reef progradation since  $\sim$ 6.5 kyr BP (Sarr et al., 2019). Similarly, Yulianto et al. (2019) found that the mangrove deposits of Belitung Island record sea level regression events dating back at least 1.5 kyr BP, implying that the coastline has prograded since then until it reached its current position. Yulianto et al. (2005) have also linked the South Kalimantan mangrove deposits to the Mid-Holocene highstand, observing a transgressive phase between 9 and 5 kyr BP and a regressive sequence since then.

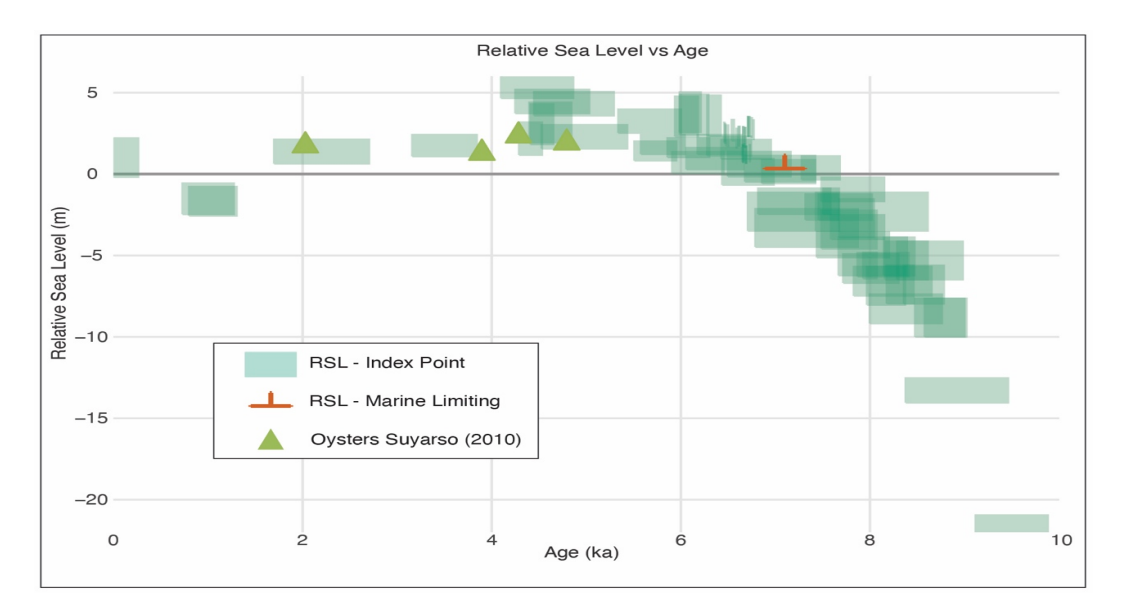


**Figure 2.** Holocene sea-level reconstruction of Belitung and surrounding areas of the Sunda Shelf derived from previous studies and records. After the compilation of Mann et al., 2019, including data from Gyeh et al., 1979; Tjia et al., 1983; Hesp et al., 1998; Scoffin & Le Tissier, 1998; Kamaludin et al., 2001; Bird et al., 2007; 2010; Scheffers et al., 2012; and Meltzner et al., 2017. We added oyster data from Suyarso (2012) but note that there are no uncertainties given. Image adapted from the HOLSEA Datahub (<a href="https://holsea-datahub-alpha.vercel.app/">https://holsea-datahub-alpha.vercel.app/</a>).

# Modern coral habitat

The fringing reef of NW Belitung Island (Fig. 1) offers a comprehensive description of the reef's flat and its coral cover. From landward to seaward, the area can be categorized into four distinct zones: the intertidal beach and mangrove, the inner reef platform, the outer reef platform, and the fore reef slope. The intertidal beach and mangrove consist of gently sloping, medium- to coarse-sandy substrates that support mangrove growth. Mangroves predominantly inhabit alluvial beach environments, where they gain relative protection and receive sediment and freshwater inputs from rivers. On the coastline, characterized by rocky shores, mangroves are absent. The inner reef platform primarily consists of sand flats, mainly calcareous materials, coral rubble, and encrusting coralline algae. Corals in this zone are sparsely distributed, primarily consisting of small colonies of Porites and Faviids. Microatolls (up to 1.5 m in diameter) were also identified in multiple locations, predominantly from the genera of *Porites sp.* The outer reef platform occurs seaward, where the reef flat is slightly raised. Here, living corals mainly consist of Acropora millepora, Acropora hyacinthus, Acropora formosa, Acropora nobilis, Montipora sp., Pachyseries speciosa, and Porites sp. (Fig. 3). The fore reef slope is characterized by a steep slope of about 30-45 degrees at a depth of about 10-15 m.

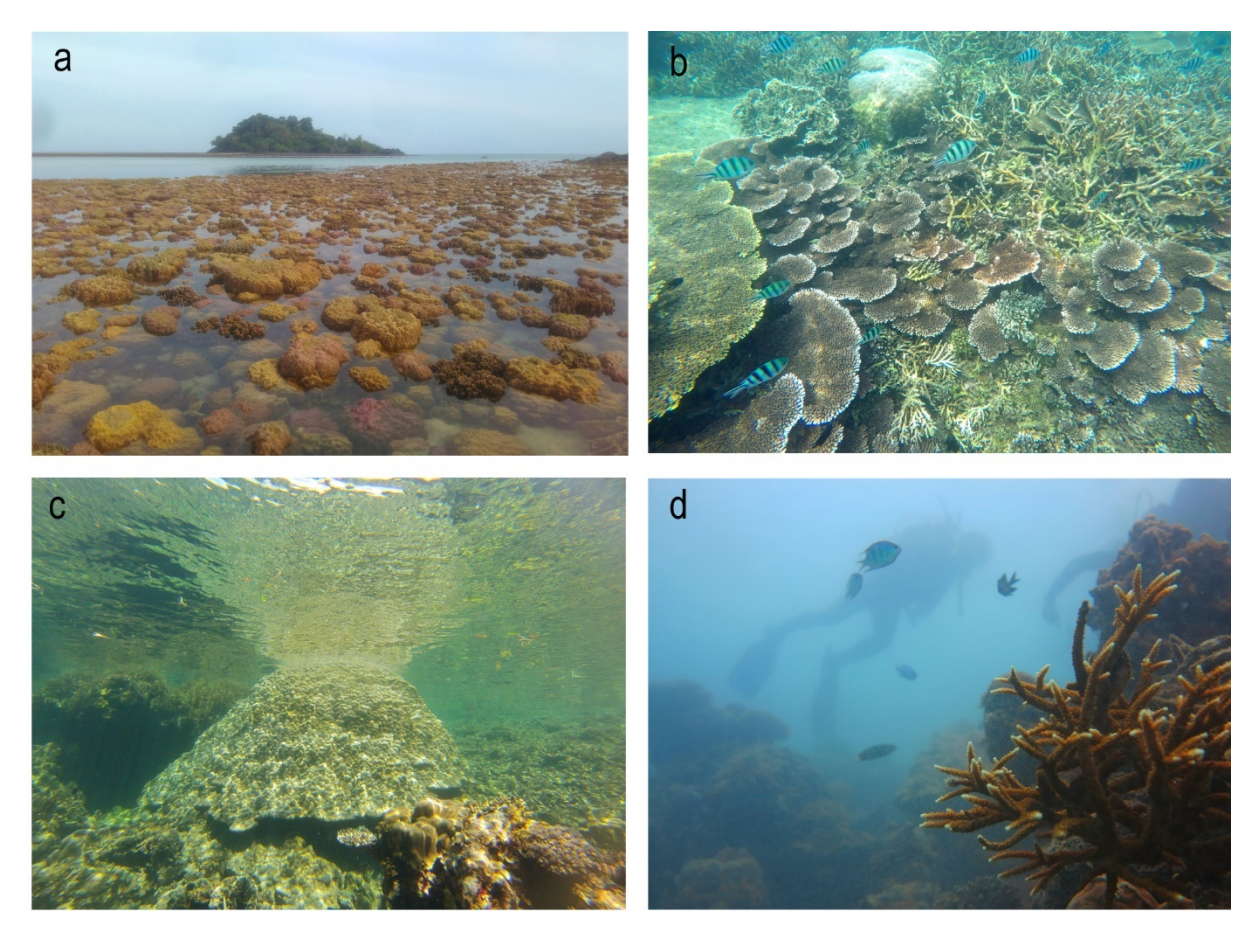


**Figure 3**. Living coral communities of the Belitung Island reefs, located around Kepayang Island (107.649495 E and 2.539065 S), include (**a**) extensive assemblages of *Porites sp.* on the outer reef platform observed during low tide, (**b**) high coral cover of mixed Acropora, mainly *A. hyacinthus* and *A. formosa*, on the outer reef platform, (**c**) domal poritids of *Porites sp.* on the outer reef platform, and (**d**) *Acropora nobilis* on the outer reef platform associated with colonies of *Porites sp.*), at depths of 3-10 m.

#### **Methods**

The distribution of reef and mangrove habitats was based on a WorldView2 image from Google Earth captured on June 25, 2021. The source image's resolution represents a ground distance of 0.6 meters. The discrimination of reef and mangrove habitats was derived from on-screen digitization and saved as ArcGIS shapefiles. Overlapping between polygons was removed, and polygons were merged and corrected. The reef and mangrove distributions were ground-truthed through direct on-the-ground observations of the study area during three different field campaigns in 2022 and 2023.

A total of ten sediment cores were collected from the study sites (Fig. 1). We obtained all cores from the mangrove habitat using a manual percussion core, as described in Solihuddin et al. (2016a; 2016b). A 3-m-long, 6.35-cm-wide galvanized metal tube with a 1.6-mm wall thickness was manually hammered into the mangrove sediment. We measured compaction on-site by subtracting the length of the penetrated core from the sediment thickness after compaction, expressed as a percentage, and corrected it by linearly scaling the core logs. The cores were split manually on both sides using a circular saw. The core site positions and elevations were fixed by DGPS (Differential Global Positioning System)

survey measurements. Longitude and latitude were calculated relative to the World Geodetic System 1984 (WGS 84), and elevations were plotted relative to the local mean sea level (MSL). The terrain profile across the mangrove habitat was based on stacked swath profiles (e.g., Fernández-Blanco et al., 2019, de Gelder et al., 2022) of FABDEM (Forest and Buildings Removed Copernicus DEM) data and shallow bathymetry from the Allen Coral Atlas (2022). FABDEM is a global elevation map that removes building and tree height biases from the Copernicus GLO 30 DEM (Neal & Hawker, 2023). The data is available at 1 arcsecond grid spacing (approximately 30 m at the equator) for the globe (https://data.bris.ac.uk/data/dataset/s5hqmjcdj8yo2ibzi9b4ew3sn). The cross-section profile from the FABDEM data was corrected vertically to the measured positions and elevations by the DGPS. The Allen Coral Atlas contains bathymetry maps at 10 m resolution, down to ~15 m depth, derived from Google Earth Engine Sentinel-2 images. They are calculated from clean coastal water mosaics, constructed over 12-month periods (Li et al., 2019).

Core logging and sampling documented characteristics including (1) sediment textural characteristics (using the Udden-Wentworth nomenclature as well as a visual assessment of sediment composition); (2) the ratio of reef framework to a matrix (after Embry & Klovan, 1971); and (3) generic coral identification (after Veron, 2000). Reef framework analysis and facies descriptions followed Montaggioni's (2005) terminology, which highlighted the growth forms of the dominant reef builders and environmental indicators.

Coral and mangrove sediments from distinct depths in each core were selected for radiocarbon dating. All coral specimens were in situ, based on orientation and skeletal condition, and free of boring, encrustation, and submarine cementation. Radiocarbon ages were obtained at the LMC14 laboratory (Saclay, France) according to their standard procedures (Moreau et al., 2013; Dumoulin et al., 2017). Radiocarbon ages were recalibrated using CALIB (<a href="http://calib.org/marine/">http://calib.org/marine/</a>) and the Marine20 calibration curve from Ramsey (2009) through <a href="https://c14.arch.ox.ac.uk/oxcal/OxCal.html#">https://c14.arch.ox.ac.uk/oxcal/OxCal.html#</a>. A weighted mean DR value of ± 70/120 (average calculation from three nearest points) was used as the best current estimate of variance in the local open water marine reservoir effect for Belitung Island and adjacent areas. We used the SHCal20 curve for organic materials (stems and roots) from mangrove sediments, since they don't have a reservoir correction. Ages discussed in the text are calibrated years before present (cal yr BP) with a 95.4% probability range.

### Results

Below, we summarize the geomorphology, contemporary habitat, facies, and accretion history of the three study sites: Sijuk, Petaling, and Batu Itam. Due to the limitations of the coring equipment and the thickness of the Holocene sedimentary facies, the Quaternary reefs, which are presumed to be present between 15 and 30 m below PMSL (Sarr et al., 2019), were not sampled. Therefore, we were unable to determine the dates of Holocene reef initiation. Below, we first describe the stratigraphy from an open mine pit in the Sijuk area, which provides a more comprehensive, 3D perspective of the different facies encountered in the cores at the other sites.

# Sijuk Open Mine Pit site

The stratigraphy of Sijuk was formerly described from observations in a drained, open mine pit (Sarr et al., 2019), where the successive facies correspond to a regressive sequence over the granitic basement (Fig. 4) that we describe here with more details. At this location

[2.552075°S, 107.804542°E], an in-situ coral reef unit is revealed by coral colonies in life position, attached to the granitic substratum (Fig. 4, D2), and by large Tridacna squamosa and meter-scale coral colonies in pristine conditions (Fig. 4, D1, Porites spp.). The outcrop does not expose the base of the unit, which, as a reefal system, likely lies at more than 20 m. A bivalve (*Tridacna squamosa*) has been dated by Sarr et al., 2019 (6,310 ± 90 yr BP). This reef is overlain by laterally varying facies, whose matrix is composed of a mix of carbonate sand and muddy clay, containing abundant corals, shells, and coralline algae (Fig. 4, C1), some of them in pristine conditions, as for instance, the numerous Cypraeidae fm. that have preserved their varnished aspect (Fig. 4, C2), indicating very low transport distances. We interpret this facies as beach deposits or shallow reef flat, ~3 m thick, with the lateral variations in the matrix reflecting local hydrodynamic conditions (directly comparable to the current, active beach). This is followed by a  $\sim$ 1 m thick facies, rich in roots and crabs (Macrophthalmus latreillei sp., Fig. 4, B2; although most fossils were found at another mine site, 800 m to the SW), characteristic of a mangrovian environment. A ~1 m thick peat unit follows, which we interpret as a possibly brackish marsh. A soil unit of variable thickness caps the sequence, covered by the Belitung rainforest.

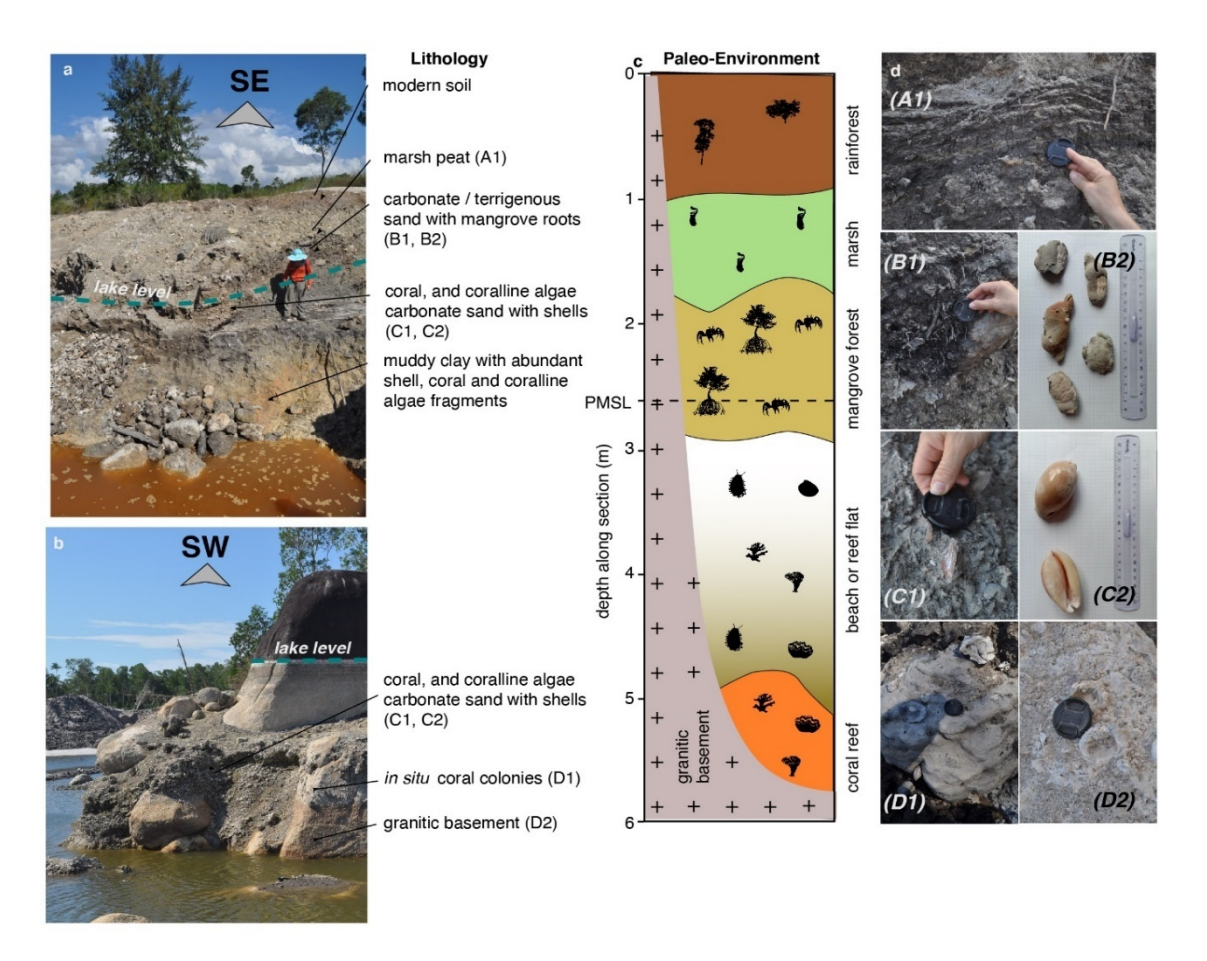


**Figure 4.** Sijuk mine pit outcrop (2015 – now inundated) showing the regressive sequence (coral reef, beach, mangrove forest, marsh, rainforest). Photographs ( $\bf a$  and  $\bf b$ ) show the lateral facies variations (water level is common datum). Identified fossils are *Macrophthalmus latreillei sp.* (B2), *Cypraeidae fm.* (C2), *Porites spp.* (D1). The reef unit has been dated to 6,310  $\pm$  90 yr BP, Sarr et al., 2019). **c)** Schematic representation of interpreted paleo-environments and **d)** Details of the various fossils.

# Sijuk site

The area of Sijuk is geomorphologically characterized by dissected hills, with the highest point reaching 60 m above sea level (Fig. 1). The coast of Sijuk is characterized by sandy beaches with low-level dune morphology on the coastal plains and a persistent sandy barrier parallel to the coastline at a few meters' elevation (Fig. 5), overlain by shrubs and coastal vegetation. Mangroves in Sijuk grow in sheltered locations, particularly in lagoon areas and river canals (Figs. 1, 5), where there is a vast, fluvial-dominated environment, according to the mangrove environmental setting from Woodroffe (1992). *Rhizopora* and *Bruguiera* are the dominant mangroves in the area, growing on an unconsolidated, brownish to blackish sand mixed with coarse to very coarse quartzite sand substrate. There are no fringing reefs along the sandy coastlines, but there are offshore patch reefs with irregular margins (rugged edges) and unbroken margins (elliptic or regular edges), measuring lengths and widths of less than 500 m and 300 m, respectively (Figs. 1, 5). The distribution of both mangroves and coral reefs is affected by irregular topographic and bathymetric features, consisting of granitic basement rock, which crop out both on- and offshore (Fig. 5).

Two cores (BN1-1 and BN1-2) were collected in the mangrove habitat approximately 2.5 km and 1 km from the coastline, respectively (Fig. 5). The elevations of the two core positions are 0.94 m and 0.76 m above PMSL, respectively. Both BN1-1 and BN1-2 have a maximum depth of 2.8 m of core penetration and 32% compaction during coring. However, Holocene sedimentary facies are significantly different between the two cores. The top ~1.25 m of BN1-1 is composed of brownish organic sand with abundant mangrove roots mixed with coarse to very coarse quartzite sand. At depths between 1.25 and 2.8 m below ground level, there are coral fragments consisting mainly of branching corals (both robust and arborescent), as well as various other genera of domal and foliaceous corals (Fig. 5). Acroporids are the most common branching corals encountered on the core, but fragments of domal coral from Porites sp. are also common, as is foliaceous coral from the genus Montipora. Muddy clay and a medium-sand matrix dominate the sediments throughout the reef section, transitioning into organic sand at the top layer. The top ~1.33 m of core BN1-2 consists of loose, coarse, brown quartzite sand mixed with organic sand with abundant mangrove roots and trunks. The rest of the core, from ~1.33 to 2.8 m deep, is made up of brown organic sand mixed with poorly sorted, medium- to coarse sand (Fig. 5).

Five radiometric ages from corals and organic materials from mangrove sediments were collected from two cores at Sijuk (Table 1). The oldest age, 6.1–5.6 kyr BP, was obtained from a coral fragment at the base of core BN1-1, about -1.83 m below present MSL. The younger age, 5.2–4.7 kyr BP, was obtained on a coral fragment from the midpoint of core BN1-1 around -0.55 m below present MSL, which yields a mean accretion rate of  $1.42\pm0.56$  mm/yr if we use  $\pm0.05$  m as depth uncertainty. The base of mangrove sediments within BN1-1 at -0.24 m below the present MSL has a radiometric age of <65 yr BP, which we attribute to young root contamination. In contrast, the ages from the BN1-2 core are much younger than the coral ages at BN1-1, showing 2.7–2.3 kyr BP and 1.7–1.3 kyr BP at -1.54 m and -0.54 m below PMSL, respectively. This value indicates an accretion rate of  $0.90\pm0.21$  mm/yr between the two samples and a rate of  $1.00\pm0.11$  mm/yr between the upper sample and the top of the core.

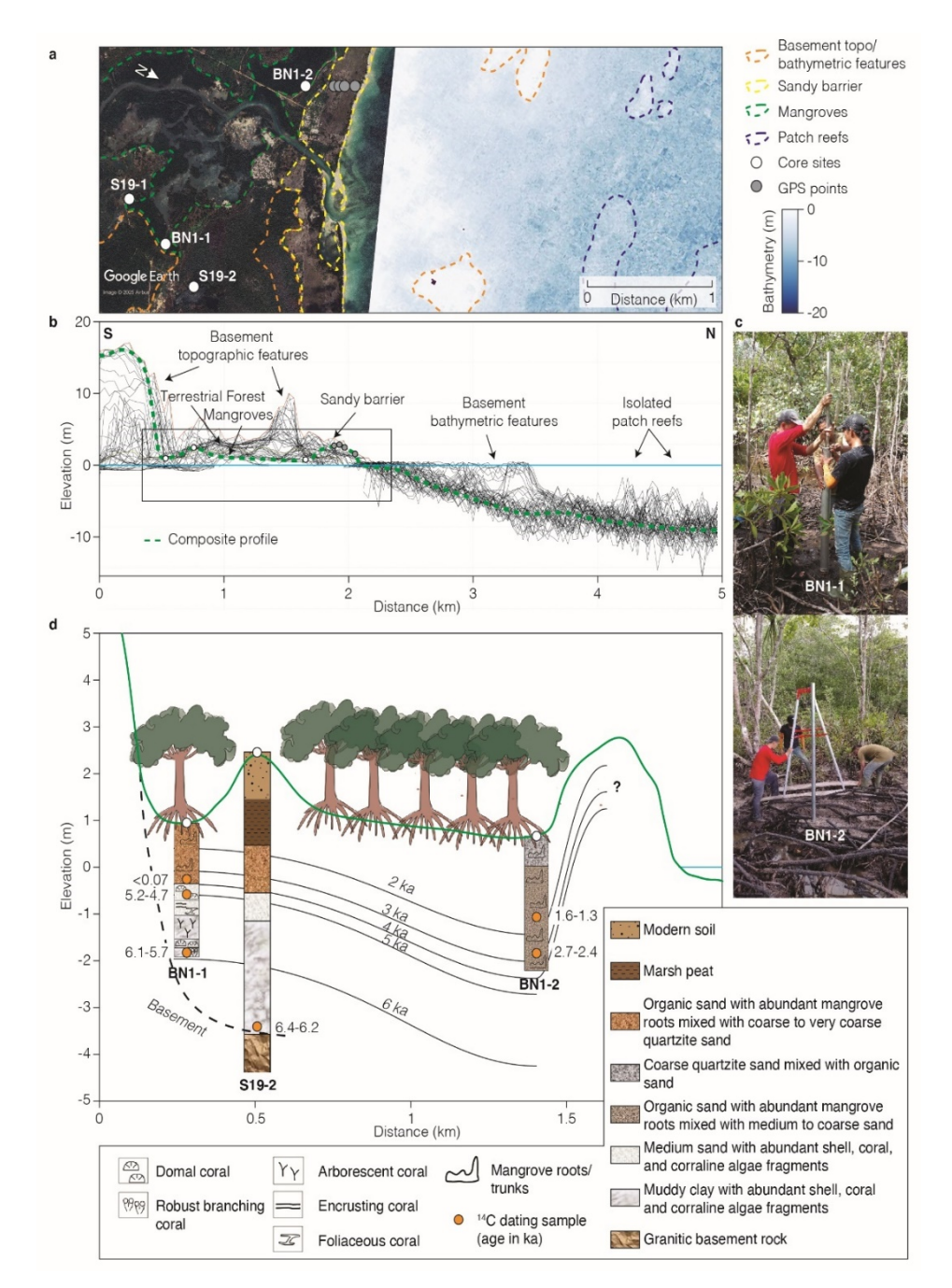


**Figure 5.** Cross-section of the Sijuk core locations with **a)** Map combining Google Earth imagery and Allen Coral Atlas bathymetry. **b)** Stacked swath profile across the map in **a** with coast-perpendicular profiles every 30 m. Composite profile combines GPS measurements with representative sections of the morphology, used in panel **d. c)** field photographs of the core sites, and **d)** isochrons based on radiocarbon dating results and a summary of the core logs that display Holocene sedimentary facies as well as the open tin mine pit at  $\sim$ 2.5 m above PMSL.

# Petaling site

Petaling is located on Mendanau Island, west of Belitung Island, and is geomorphologically characterized by highly dissected hills, with the highest point reaching 80 m above mean sea level (Fig. 1). The coast of Petaling is predominantly characterized by mangrove habitat, with

narrow fringing reefs and scattered patch reefs offshore (see Figs. 1, 6). Petaling's mangroves densely grow along the coast, where there is a wide (up to 0.5 km) low-gradient intertidal zone suitable for mangrove colonization (Woodroffe, 1992). *Rhizophora* and *Avicennia* are the dominant mangroves in the area, which sit on unconsolidated, dark brownish organic sand mixed with poorly sorted, medium- to coarse sand substrates. The reef flat is mostly occupied by sand sheets and coral rubble. Irregular topographic features consisting of meta-sandstone basement rocks crop out onshore (Fig. 6), affecting the distribution of mangroves. The patch reefs offshore seem to occur along a bathymetric high that is the continuation of an island to the NNE (Fig. 1).

Four cores (BN2-1, BN2-2, MEN-3, and MEN-4) were taken in the mangrove habitat approximately 0.1, 0.5, 1.0, and 1.5 km from the coastline, respectively (Fig. 6). The maximum depths of BN2-1, BN2-2, MEN-3, and MEN-4 core penetration are 2.7 m, 1.46 m, 1.7 m, and 1.54 m, and compaction during coring was 37%, 20%, 32%, and 34%, respectively. The Holocene sedimentary facies of BN2-1, BN2-2, and MEN-4 are very similar. They have a top layer of loose, dark brownish organic sand with many mangrove roots and trunks mixed in with poorly sorted, medium- to coarse sand and a bottom layer of metasandstone rock. For BN2-1, BN2-2, and MEN-4, the lithological contact between unconsolidated organic sand and basement rock is 1.85 m, 1.09 m, and 1.46 m deep below ground, respectively. The top section of MEN-3, situated approximately 20 m from BN2-1, consists of organic sand, while a coral reef layer lies beneath it at a depth of 85 cm below ground (Fig. 6).

Five radiometric dating samples were obtained from 1 coral sample and 4 organic materials from mangrove sedimentary layers collected from three cores at Petaling (Table 1). Out of the 4 sediment layers, 3 were <70 yr BP and probably erroneous due to young root contamination. Radiocarbon dates from BN2-1, obtained from samples taken at -1.69 m below PMSL, show an age of 471–132 yr BP, and from MEN-3, taken at -1.73 m below PMSL, reveal an age of 4.3–3.8 kyr BP.

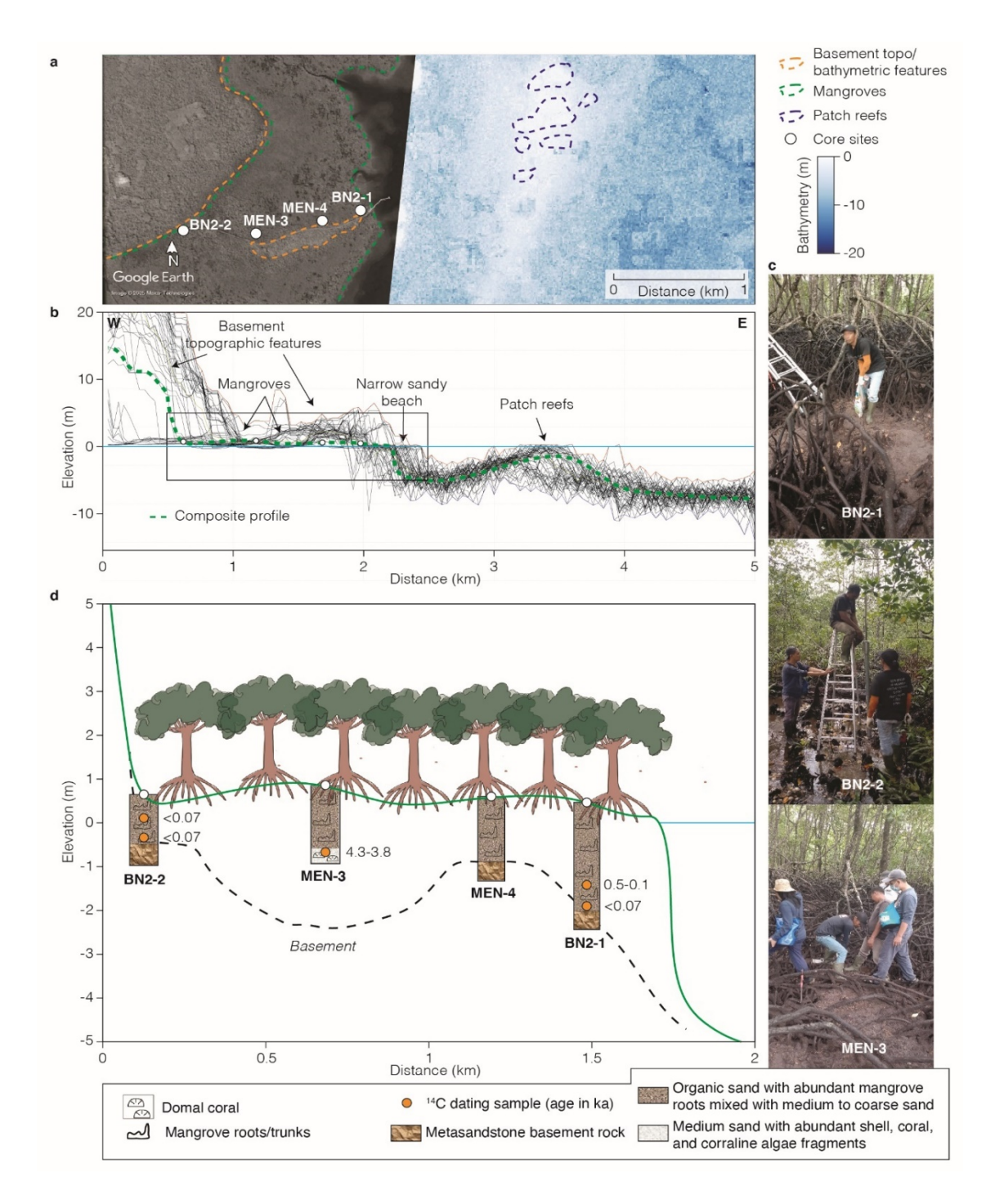


**Figure 6.** Cross-section of the Petaling core locations with **a)** Map combining Google Earth imagery and Allen Coral Atlas bathymetry. **b)** Stacked swath profile across the map in **a** with coast-perpendicular profiles every 30 m. Composite profile combines GPS measurements with representative sections of the morphology, used in panel **d. c)** field photographs of the core sites, and **d)** summary of the core logs that display Holocene sedimentary facies.

# Batu Itam and Temparan sites

Batu Itam is located on the NW coast of Belitung Island and is geomorphologically characterized by highly dissected undulating plains of denudational origin, with the highest point reaching 40 m above PMSL (Fig. 1). The coast of Batu Itam is predominantly

characterized by mangrove habitat along the shore with an extensive intertidal fringing reef and scattered patch reefs offshore (see Figs. 1, 7). *Rhizophora* and *Avicennia* are the dominant mangroves in the area, sitting on unconsolidated brownish to blackish sand mixed with a coarse to very coarse quartzite sand substrate. The reef flat, which stretches approximately 2.3 km seaward, is composed of carbonate sand, coral rubble, encrusting coralline algae, encrusting corals, microatolls (up to 1.5 m in diameter), sparsely small living coral colonization, and predominantly *Thalassia* seagrass with a height of 10–15 cm. The reef flat has slightly emerged on the reef crest, forming a ridge morphology on the reef edge.

Six cores (BN3-1, BN3-2, BN3-3, BN3-5, BN3-6, and BN3-Al) were taken on the mangrove habitat at two different coast sections, including three cores (BN3-1, BN3-6, and BN3-Al) at Batu Itam (Fig. 7) and three cores (BN3-2, BN3-3, and BN3-5) at Temparan (Fig.7). The maximum depths of BN3-1, BN3-2, BN3-3, BN3-5, BN3-6, and BN3-Al core penetration are 2.85 m, 1.35 m, 1.56 m, 1.06 m, 1.04 m, and 0.8 m, and compaction during coring was 35%, 19%, 49%, 41%, 24%, and 13%, respectively. The Holocene sedimentary facies of BN3-3, BN3-5, BN3-6, and BN3-Al are quite similar. They consist of a thin layer of loose, brownishto-blackish organic sand with many mangrove roots at the top 0.2 m. Below the organic sand is coral reef facies, comprising arborescent, robust branching, and dome-shaped corals with an unconsolidated, brownish-gray, sandy matrix. The branching coral clasts on BN3-3, BN3-5, BN3-6, and BN3-Al are mostly made up of arborescent and robust acroporids. However, the bottom section of the BN3-6 core also contains domal coral from the genus Porites sp. (Fig. 7). BN3-1 and BN3-2 are exceptions. BN3-1 consists of unconsolidated dark grey, very fine to fine sand with shell fragments, gastropods, mollusks, rock fragments, and roots at the base; a thin layer of unconsolidated coarse quartzite sand mixed with blackish organic sediment; and a top layer of unconsolidated dark brownish organic sediment mixed with fine to coarse quartzite sand. BN3-2 consists of organic sand at the top and basement rock at the bottom (Fig. 7).

Six radiometric ages were obtained from corals collected from Batu Itam (Table 1). The base of BN3-6 yielded the oldest age, 5.9-5.4 kyr BP, approximately -0.97 m below present MSL. The base of core BN3-5 (-0.1 m below present MSL) and BN3-Al (-0.56 m below present MSL) recorded relatively similar ages of 5.5-5.1 kyr BP and 5.1-4.5 kyr BP, respectively. The upper layer of the BN3-Al core is the youngest age, 5.0-4.5 kyr BP, approximately -0.1 m below present MSL. The upper layers of BN3-6 (-0.3 m below present MSL) and BN3-5 (+0.15 m above present MSL) recorded a relatively similar age of 5.0-4.5 kyr BP and 5.5-5.0 kyr BP, respectively. Thus, the accretion rates of BN3-Al, BN3-6, and BN3-5 were  $5.7 \pm 25$  mm/yr,  $0.81 \pm 0.35$  mm/yr, and  $4.3 \pm 22$  mm/yr, respectively. One radiometric age from organic materials from mangrove sediments collected at Batu Itam (BN3-2) was <70 yr BP and is likely erroneous due to young root contamination. (Table 1). The other one at BN3-1 was also young but possibly more reliable, with a calibrated age of 251-504 BP (Table 1).

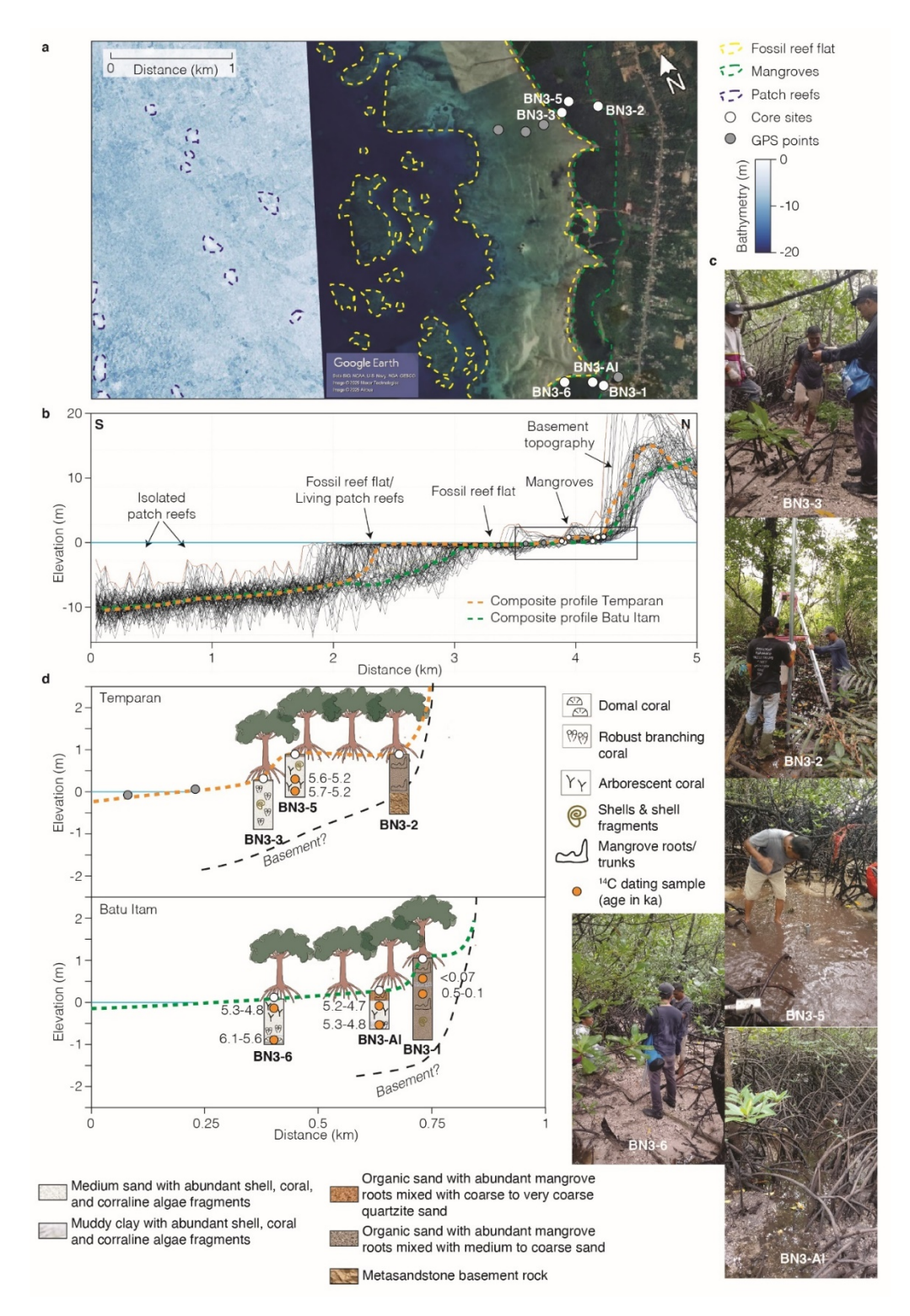


**Figure 7.** Cross-section of the Temparan and Batu Itam core locations with **a)** Map combining Google Earth imagery and Allen Coral Atlas bathymetry. **b)** Stacked swath profile across the map in **a** with coast-perpendicular profiles every 30 m. Composite profile combines GPS measurements with representative sections of the morphology, used in panel **d. c)** field photographs of the core sites, and **d)** summary of the core logs that display Holocene sedimentary facies.

**Table 1.** Radiocarbon dates from coral and organic materials from mangrove sediments across study sites. Calibrated age represents a 95.4% confidence interval.

Site	Sample Code	Lab code	Material	Elevation relative to PMSL (m)	Delta C13	Conventional age (BP)	Calibrated age (cal yr BP)
Sijuk	BN1-1 (24-29)	SacA68616	Mangrove sediments	0.38	-30.7	After 1950	<70
	BN1-1 (55-58)	SacA68606	Coral	0.12	-3.2	4805 ± 30	5245-4724
	BN1-1 (183-185)	SacA68607	Coral	-1.76	-4.3	5630 ± 30	6118-5665
	BN1-2 (87-91)	SacA68617	Mangrove sediments	-0.55	-35.7	1525 ± 30	1587-1302
	BN1-2 (155-160)	SacA68618	Mangrove sediments	-1.55	-34.2	2495 ± 30	2754-2364
Petaling	BN2-1 (55-59)	SacA68619	Mangrove sediments	-1.44	-28.3	215 ± 30	471-132
	BN2-1 (82-86)	SacA68620	Mangrove sediments	-1.96	-30.0	After 1950	<70
	BN2-2 (40-44)	SacA68621	Mangrove sediments	0.51	-28.2	After 1950	<70
	BN2-2 (66-69)	SacA68622	Mangrove sediments	0.25	-27.2	After 1950	<70
	MEN-3 (OSL base)	SacA70699	Coral	-0.75	-4.5	4120 ± 30	4337-3826
Batu Itam & Temparan	BN3-1 (75-82)	SacA68624	Mangrove sediments	-0.3	-26.6	215 ± 30	251-504
	BN3-2 (58-61)	SacA68625	Mangrove sediments	0.1	-30.6	After 1950	<70
	BN3-AI (20)	SacA68604	Coral	0.0	1.1	4790 ± 30	5238-4711
	BN3-AI (80)	SacA68605	Coral	-0.68	-1.4	4870 ± 30	5289-4822
	BN3-5 (4-11)	SacA68608	Coral	0.72	-6.7	5225 ± 30	5676-5257
	BN3-5 (29-33)	SacA68609	Coral	0.32	-1.7	5295 ± 30	5742-5308
	BN3-6 (8-10)	SacA68610	Coral	-0.07	-6.8	4830 ± 30	5270-4786
	BN3-6 (75-78)	SacA68611	Coral	-0.97	-2.4	5590 ± 30	6094-5621

All samples were dated at Laboratoire de Mesure du Carbone 14 (LMC14; Saclay, France)

# **Discussion**

# Sedimentary facies and accretion

We identified two distinct facies based on their constituent materials: coral and mangrove facies. Coral facies are situated directly below the mangrove facies, with no terrigenous sediment layer in between. In terms of paleoenvironments described in Fig. 4, they would

correspond to either a coral reef or the beach/reef flat. Mangrove facies are situated either on top of coral facies or directly on top of basement rock types (granites or meta-sandstone). In terms of paleoenvironment (Fig. 4), they correspond to a mangrove forest.

The coral facies are characterized by the presence of carbonated skeletons and grains that originate from the coral reef environment. The composition comprises four primary subfacies: domal, robust, arborescent, and folliaceous. Most of the coral fragments are fresh and seem to be in their original position, as evidenced by their growth orientation and well-preserved skeletal structure. The ages of these coral facies range from ~6 kyr BP (BN1-1, BN3-6) to ~4 kyr BP (MEN-3), but older bivalve samples have been reported by Sarr et al. (2019; 7.3-6.3 kyr BP) at the Sijuk site. The matrix sediment composition varies between Sijuk and Batu Itam. At Sijuk, the matrix sediments are almost evenly split between poorly sorted medium sand and muddy clay (see Fig. 5). At Batu Itam, however, the matrix sediments are primarily composed of poorly sorted medium sand. This suggests that they had distinct depositional environments during the Holocene, indicating that Sijuk had a more sheltered reef environment, whereas Batu Itam had more exposed surroundings with higher wave energy.

- Domal coral sub-facies are dominated by dome-shaped poritids (mostly *Porites sp.*). On Belitung Island, domal coral sub-facies in a sandy matrix is more prevalent at Sijuk. As postulated (Done, 1982; Cabioch et al., 1999; Grossman & Fletcher, 2004; Montaggioni, 2005; Hibbert et al., 2016), domal coral colonies tend to occupy lower-energy reef settings, from surface to depths of around 10–15 m. This observation strongly suggests that the domal coral sub-facies on Belitung Island has formed in a semi-exposed, sheltered paleoenvironment. Here, the sub-facies inhabits a nearshore environment and relict reef flats and is relatively located in the upper part of the reef section.
- Robust-branching coral sub-facies are dominated by acroporids from the genera of Acropora *formosa* associated with domal poritids (*Porites sp.*). On Belitung Island, the distribution of robust-branching coral colonies in a sandy matrix is more common at Batu Itam. They are located in a relatively shallow paleoenvironment, with water depths of less than ~2 m in most of the sampled cores. Similar to this, Montaggioni's (2005) description of the Indo-Pacific robust-branching coral facies suggests that this facies occurs in relatively high-energy, very shallow (0–6 m deep) water and is widely distributed on the outer reef flat to the upper fore reef zones.
- Various thin-branched corals dominated by acroporids form arborescent-branching coral sub-facies on Belitung Island. The cores of both Sijuk and Batu Itam contain these sub-facies. At Sijuk, this facies disperses in a muddy clay matrix in relatively deeper water (~2–2.5 m), while at Batu Itam, it disperses in a medium sand matrix at a depth of less than 1 m. These grains are primarily produced by corals, molluscs, and foraminiferal tests. The relatively shallow subtidal distribution of arborescent-branching coral sub-facies on Belitung Island is likely a function of its low tolerance to subaerial exposure, which also excludes such coral communities on the contemporary reef flat (Solihuddin et al., 2015). The type of coral resembles Montaggioni's (2005) description of arborescent coral, which usually grows in areas that are partly exposed or partially protected at depths of less than 20 m, as well as on shallow inner reef flats and back reef slope zones (Hopley et al., 2007).
- Foliaceous coral sub-facies is encountered on the upper part of the Sijuk core at a depth of approximately 1.5–2 m below ground (see Fig. 5). The coral clasts primarily consist of platy *Montipora sp.* colonies embedded in an unconsolidated dark gray

medium sand matrix, which also includes coral debris, gastropods, bivalves, and foraminifera tests. Montaggioni (2005) found similar patterns in the Holocene reef sections of the Indo-Pacific regions. These patterns show that the foliaceous coral facies grows in protected reef environments that usually have a lot of suspended sediment (Takahashi et al., 1988; Kleypas, 1996; Montaggioni & Faure, 1997). This facies is frequently colonized by arborescent coral communities in water depths of less than 15 meters (Done, 1982; Woesik & Done, 1997; Yamano et al., 2001).

The mangrove facies is either distributed above the coral facies or basement rock, with a thickness of up to 2.5 m. The facies can be found in Sijuk, Petaling, and Batu Itam, but the mangrove densities are very different in each place. It is made up of loose, brownish to blackish organic sand that has many mangrove roots in it. Mangroves appear to thrive in conditions of optimal wave energy. At present-day, Belitung remains in a quiet environment, with low wave energy and height. At all locations, wave heights very seldom exceed 0.8 m, but modest variations in wave energy appear between sites (https:// ihnienhuis.users.earthengine.app/view/changing-shores). The low wave energy at Petaling (~0.4 J/m²) facilitates more extensive progradation of mangroves over fossil reefs and eroded basement compared to Batu Itam, which has a slightly higher wave energy (1.7 J/m²) and features a relatively narrow mangrove forest. Offshore Sijuk, wave energy reaches 2.8 J/m<sup>2</sup>, predominantly from the northern direction, i.e., a higher energy environment that could prevent the development of low-energy coral colonies. However, the waves promoted the establishment of extensive sandy barriers, which are currently overlain by dunes (see Fig. 5), creating a relatively calm environment conducive to the development of lagoonal reefs and mangroves. The ages span from the Late Holocene (2.7-2.3 kyr BP) to the near past (471–132 yr BP) (Table 1). The modern mangrove types are dominated by Rhizophora, Bruguiera, and Avicennia, sitting on the relict reef flat and/or basement rock.

Apparent accretionary rates appear similar for coral reef system deposits compared to mangrove deposits (Fig. 8), although we have only one site with multiple reliable mangrove deposit ages, and we cannot be completely sure that the ages of the coral samples are the same as the ages of deposition. Taking the ages at face value, accretion rates for coral fragments range from  $0.8 \pm 0.4$  mm/yr to  $5.7 \pm 25$  mm/yr. The corals at the higher elevation, between ~0.6 below MSL and ~0.7 m above MSL, from Batu Itam (BN3-AI) and Temparan (BN3-5), showed the fastest accretion rates (Fig. 7). This phase is likely to occur as the coral rubble accumulates on the swash zone (foreshore), extending from mean low tide to mean high tide under moderate to high energy (Short, 2012). The mangrove accretion rate for BN1-2 is  $0.9 \pm 0.2$  mm/yr between ~2.5 and ~1.5 kyr BP and a very similar 1.0  $\pm$  0.1 mm/yr between ~1.5 kyr BP and the present (top of the core). The younger samples, from BN2-1 and BN3-1, indicate much higher rates of  $6.3 \pm 3.6$  mm/yr and  $3.2 \pm 1.1$  mm/yr, respectively. Larger compilations also reveal similar discrepancies. Modern fringe-type mangrove forests show ranges from a low of 1.6 mm/yr to a high of 8.6 mm/yr (Woodroffe et al., 2014), a range that our rates for BN2-1 and BN3-1 fall well within. A global compilation of 78 Holocene mangrove sequences showed ranges of ~0.2–2.0 mm/yr vertical accretion rates for the past 6 kyr BP (Saintilan et al., 2020), a range that our accretion rates for BN1-2 fall well within. One reason for these discrepancies could be that mangroves are very dynamic in terms of sedimentary settings, where periods of rapid deposition may alternate with periods of erosion (e.g., Nathan et al., 2025), and the short-term rates over a few hundred years are not necessarily representative of Holocene rates. Another reason might be that the BN2-1 and BN3-1 mangrove sediment samples have been contaminated as well by younger roots, as for several of the samples dated <70 years (Table 1). To resolve such differences in

future work, we have taken samples from the same sediments for optically stimulated luminescence (OSL) dating.

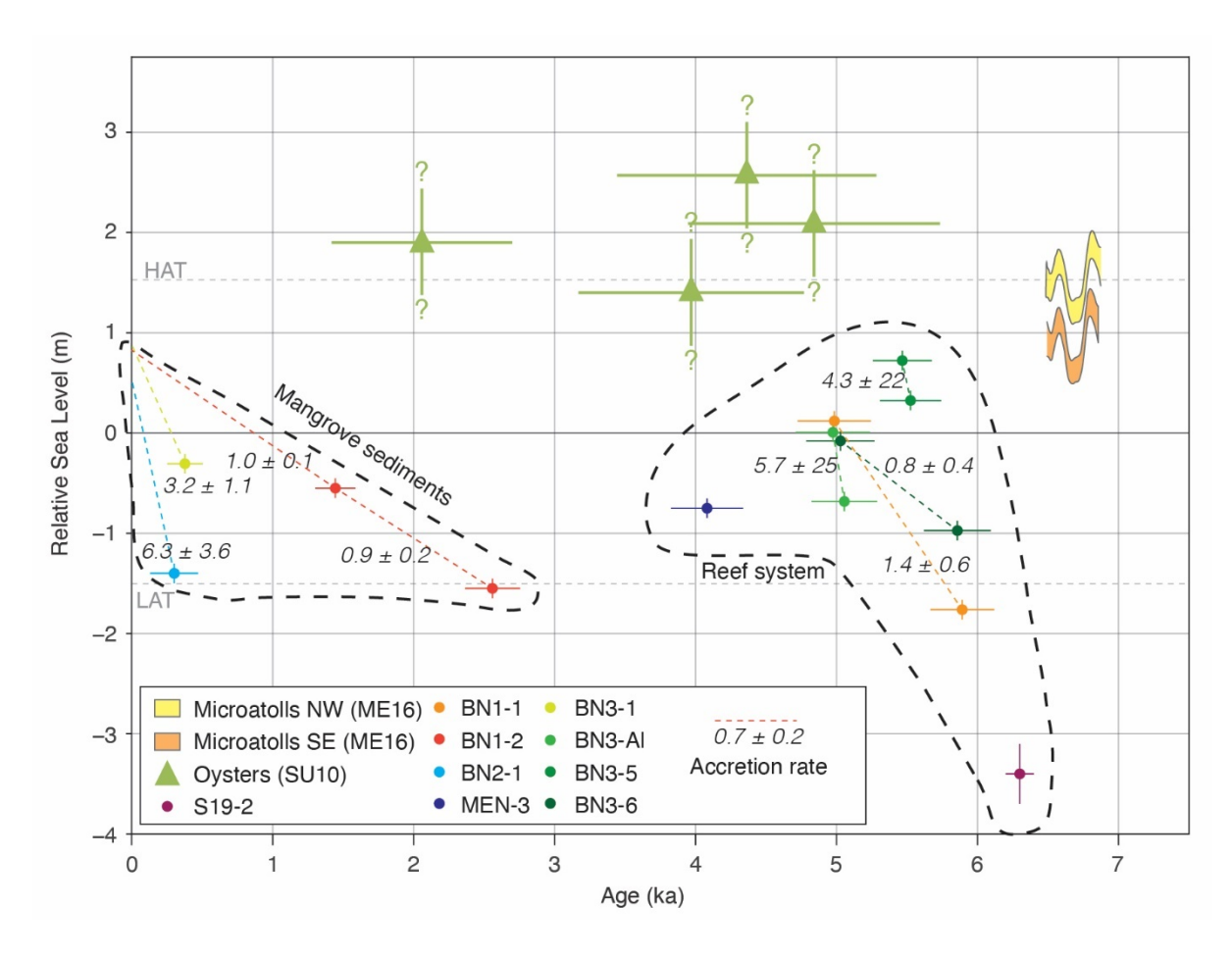


**Figure 8.** Dated core samples with their elevation relative to PMSL, and apparent accretion rates, compared to relative sea-level estimates for Belitung Island derived from microatolls (Meltzner et al., 2017) and oysters (Suyarso, 2012, vertical uncertainty not mentioned). HAT = Highest Astronomical Tide and LAT = Lowest Astronomical Tide are represented with grey dashed lines. Accretion rates for mangrove samples (BN1-2, BN2-1, BN3-1) are calculated assuming the ages of the cores tops were 0 yr.

#### Chronology of Holocene coral reef and mangrove interplay

On Belitung Island, we divide the chronology of the Holocene coral reef system (including the reef *per se* and the onshore beach deposits) and mangrove buildup into two phases: nearshore reef establishment and mangrove development show that these two regimes closely reflect relative sea level variations.

The Holocene sea-level curve for the Sunda Shelf (Fig. 2) indicates that the reef established shortly after rising sea levels inundated the antecedent substrates, around 6.5 kyr BP (Fig. 8). Relative Sea Level (RSL) estimates for Belitung from microatoll data (Meltzner et al., 2017) are 4–6 m above the coral sample of S19-2 of comparable age (Fig. 8), suggesting the sampled reef in Sijuk was growing at several meters' water depth around 6.5 kyr BP. Both regional paleo sea-level indicators (Fig. 2) and the Belitung oyster fossils of Suyarso (2012; Fig. 8) suggest elevated mid-Holocene sea-level (>2 m above PMSL) persisted until

around  $\sim$ 4.5 ka. Although Suyarso (2012) did not provide error margins, we expect those to be within a few 10s of cm, given that 1) oysters usually live between mean sea level and the highest tide during neap tide (Hopley et al., 2007), which is  $\pm$  15-30 cm in Belitung, and 2) in the field we typically observed living oysters within  $\sim$ 30 cm above and below PMSL. This implies that the  $\sim$ 4-6 ka corals dated in this study, deposited between  $\sim$ 0.8 m above and  $\sim$ 1.7 m below PMSL, were probably part of a reef flat (Petaling, Batu Itam, Temparan) or shallow lagoon (Sijuk).

In general it seems that during the period of ~6.5 kyr BP to ~4 kyr BP the reef around Belitung was aggrading, with 1) a consistent age-depth decrease in Sijuk for S19-2 and core BN1-1, from  $\sim$ 6.3 kyr BP at  $\sim$ 3.5 m below PMSL (S19-2) to  $\sim$ 5 kyr BP at  $\sim$ 0.5 m below PMSL (Fig. 4), 2) reef infill occurred between the basement topography in Petaling until ~4 kyr BP (Fig. 6), and 3) similar ages of ~5 kyr BP were found at ~0.2 m below PMSL between BN3-Al and BN3-6 over a distance of a few hundred meters in Batu Itam (Fig. 7). On top of aggradation, some progradation also has occurred, especially in Sijuk, where a former lagoon was progressively filled with reef and mangrove sediments (Fig. 5). Other than attesting to sedimentary progradation, the depth of the  $\sim$ 2.5 ka mangrove sediments at  $\sim$ 1.5 m below PMSL also implies that relative sea level must have been close to present-day elevations by that time, given the ± 1.5 m intertidal range providing mangrove habitat (Fig. 8). The sandy barrier in Sijuk was likely established around 2.5 ka, as the wave energy along the north coast precludes the existence of present-day fringing mangroves, and oceanographic conditions have probably remained stable since the mid-Holocene (Meltzner et al., 2017). Given the lack of ages on the sandy barrier, we don't know when it started to form, but the river morphology, curving eastward while passing through it (Fig. 5), suggests the barrier has also been prograding eastward, consistent with the strong west monsoon on Belitung (Pamungkas, 2018).

The relative sea-level fall between ~4 and ~2.5 kyr BP probably marked the onset of mangrove extension around Belitung. At all cross-sections, the reef that had formed in the few thousand preceding years could then provide a low-sloping substrate in the intertidal zone, which was no longer suitable for most coral species to grow given the occasional subaerial exposure but ideal for mangroves. Although we don't have the ages of the oldest mangrove sediments directly above the reef system deposits, we note that comparable mangrove deposits on Sungai Padang, Belitung (~25 km eastward from Sijuk), reported by Yulianto et al. (2019), recorded events of sea level regression dating back to at least 1.5 kyr BP. In Petaling and Sijuk, prograding mangroves have completely covered mid-Holocene reef flats, but in Batu Itam and Temparan, this process is still ongoing, as attested by pioneering *Rhizophora* mangroves that appear seawards of the mangrove forest on the fossil reef flat (Fig. 9). Living reefs have migrated seawards since the relative sea-level fall, and they are now mostly found as isolated patch reefs, both close to the shoreline and up to a few km seawards (Figs. 1, 5-7). We've illustrated the Holocene coastal landscape evolution of the Batu Itam and Temparan sections in Fig. 9.

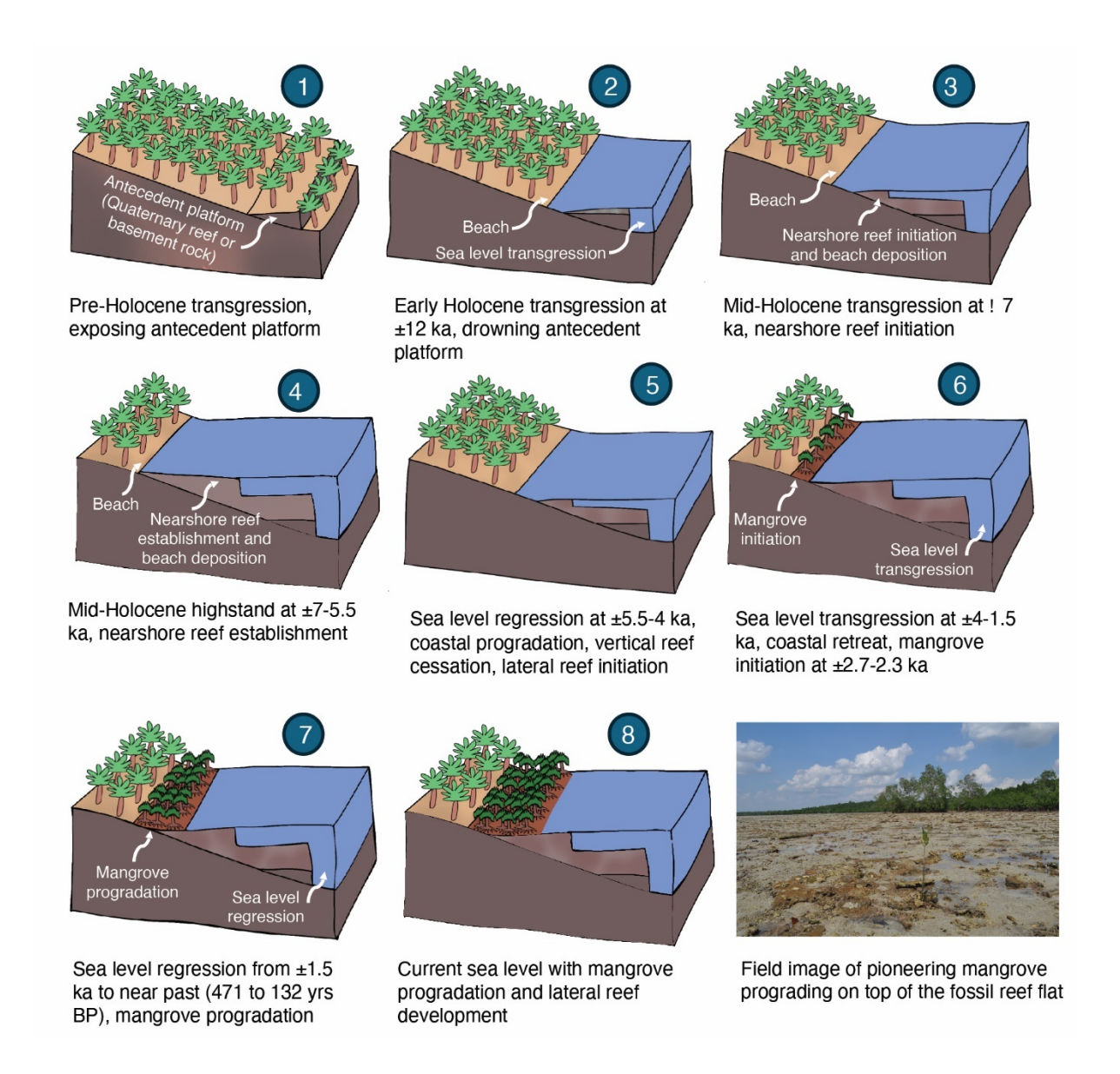


**Figure 9.** Coastal landscape evolution from early Holocene to current conditions showing chronology of Holocene coral reef and mangrove interplay for the Batu Itam & Temparan sections. Modified from Erkan & de Gelder (2025).

The three coastal sections analyzed in this study provide some key similarities and differences. The most striking similarity between the three coastal sections is that the geological evolution of the early-mid Holocene reef system has been pivotal to the subsequent development of mangrove forests. It calls into question to what extent this is a generic characteristic for Holocene tropical coastline evolution on the larger scale. With the exception of the N-Caribbean region, most of the world's tropical coastlines experienced a mid-Holocene highstand with (slow) relative sea-level fall since then (Khan et al., 2015). It would make sense that a lot of mangroves on those coastlines, in particular the 'open coast' (e.g., Worthington et al., 2020) or 'fringing' (e.g., Kathiresan, 2021) type mangroves like in Petaling, Temparan, and Batu Itam, benefitted from prior Early to Mid-Holocene reef formation, allowing for a vast expansion during relative sea-level fall. Yet this geological preconditioning has so far been largely ignored in studies on Holocene mangrove evolution. In the case of deltaic and estuarine type mangroves, the Mid- to Late Holocene sea-level fall

seems to have had opposite effects, with decreased mangrove occupation in large river systems in Vietnam, Australia, and Cambodia (Thom et al., 1975; Woodroffe et al., 1985; Tanabe et al., 2003; Woodroffe et al., 2005). At these locations the accretion and progradation of delta systems led to an increase in salt marshes, freshwater wetlands, and terrestrial forests at the expense of mangroves (Saintilan et al., 2020). Interestingly, this also seemed to have happened in Sijuk at a much smaller scale, as the mangrove sediments in the open minepit (S19-2; Figs 4-5) are overlain by peat deposits and modern terrestrial forest soil. The location of S19-2, where mangroves used to be present, is almost ~1 km away from the current mangrove limit, suggesting the mangrove extent has been strongly reduced as sediments filled in the former lagoon/estuary during relative sea-level fall.

There is a main difference in wave energy between the three sites (see previous section), which dictated the coastal morphology: a sandy barrier with river channel/estuarine mangroves for the highest wave energy environment (Sijuk, Fig. 5) and fringing reefs with open coast mangroves for the lower wave energy environments (Petaling, Batu Itam, and Temparan, Figs. 6-7). Furthermore, we propose that the lower wave energy in Petaling, compared to Batu Itam and Temparan, allowed the mangroves to fill up all the available accommodation space until the shoreline (1-2 km; Fig. 6), whereas in Batu Itam, only around 25% of the intertidal flat is occupied by mangroves (~300–400 m; Fig. 7). There may be a difference in sediment supply between Petaling and Batu Itam/Temparan, but we don't see clear reasons for that. Other differences between the sections include the presence of basement topographic and bathymetric features that are more pronounced in Sijuk and Petaling, although in all cases the basement topography puts a sharp landward limit on the spatial extent of the mangrove forests.

The future of Belitung's coral reefs and mangroves during 21st-century relative sea-level rise will depend on several factors, including reef growth conditions, sediment aggradation, temperature changes, wave erosion, monsoon changes, and oceanographic conditions. For the open coast mangroves on Belitung, there appears to be little accommodation space landward, with the basement topography sharply increasing at the current mangrove limits (Figs. 6-7). As such, both sediment aggradation rates and vertical reef growth rates will probably have to match rates of relative sea-level rise (RSLR) if they are to maintain their surface area. If aggradation rates are lower, mangroves will eventually drown. If reef growth rates are lower, water depths will increase, which will likely increase wave erosion of the mangroves. RSLR rates for nearby Singapore are predicted to rise to ~4, ~8, and ~12 mm/ yr by the year 2100 under Representative Concentration Pathway (RCP) scenarios 1.9, 4.5, and 8.5, respectively (Shaw et al., 2023). Although the limited ages and aggradation rates obtained in our study are subject to high uncertainties (Fig. 8) and might not be representative of the near future under different conditions than the mid-Holocene, none of them are as high as the rates associated with the mid- and higher RCP scenarios, leaving little room for optimism about the future of the Petaling, Batu Itam, and Temparan mangroves. The case of Sijuk is different, in the sense that the sandy barrier is several meters above PMSL and can shield the mangroves behind it from increased wave energy. Furthermore, most of the terrestrial forest that developed on top of the mangrove sediments around S19-2 has its ground level at ~2-3 m elevation (Fig. 5), which would potentially allow mangroves to partially re-accommodate those vast areas under the different RSLR scenarios.

Global compilations of Holocene mangrove sites suggest most mangroves could only develop when RSLR fell below ~7 mm/yr (Saintilan et al., 2020, 2023) in the Early to Mid Holocene. Modern-day sea level rise is currently estimated around 4 mm/year, and it is estimated to increase in the following decades (Rahmstorf, 2007; Cazenave & Llovel, 2010;

Mitchum et al., 2010; IPCC, 2021). Although we imagine these RSLR rates will provide severe challenges to the survival of mangrove forests, we also emphasize that the starting point will be very different this time around. Just like the early- to mid-Holocene coral reef systems preconditioned a suitable mangrove substrate, undoubtedly affecting RSLR thresholds for mangrove growth in that period, the current period of sea-level rise is developing on top of a more complex Holocene coastal geomorphology that evolved over a longer period of time. As such, RSLR thresholds for mangrove survival will likely be very context dependent, in terms of mangrove type, like the open coast and river estuarine mangroves in this study, but also in terms of geological pre-conditioning. In line with the concept of biogeomorphological inheritance (Woodroffe, 2025), we propose that characterization and quantification of Holocene reef growth, mangrove formation, sedimentation, and wave erosion in relation to coastal evolution may provide key insights to a tailored anticipation of future RSLR scenarios in mangrove preservation strategies.

#### Conclusion

This case study from Belitung Island, Indonesia, offers a new insight into the interplay between coral reefs and mangroves in response to the Holocene sea-level changes. We relate distinct sedimentary facies, including mangroves and deposits from the adjacent coral reef system, as well as the chronology of their development, itself tied to sea level changes. The Holocene sea-level rise led to the establishment of nearshore reefs on Belitung Island from ~6.5 to ~4 kyr BP at an elevation between ~1.8 m below PMSL and 0.8 m above PMSL. Following the formation of the nearshore reef and subsequent sea level fall, mangroves benefitted from the now-abandoned reef flat to develop and prograde seaward since at least the Late Holocene (2.7–2.3 kyr BP) until present-day, with a thickness of more than 2.5 m in the sheltered Sijuk area and up to 2 m at the open-coast sites in Petaling.

Current findings contribute to our understanding of the geological and ecological processes that influence coastal ecosystems, providing insight into the complex interaction between coral reefs, mangroves, and sea level changes throughout geological periods and the anticipated sea level rise on coastal ecosystems by the 21st century. Reef growth rates, sedimentation rates, and wave energy all contribute to the historical and future development of the coastline, but sea level oscillations as modest as the Mid- to Late Holocene are even more critical for the determination of morphology on which coral reefs and mangroves develop. The extensive stretches of open coast mangroves in the modern world could often owe their dimensions to the Mid-Holocene development of coral reefs that converted during the Late Holocene regression into large flats opportune to the expansion of mangrove forests.

The fate of mangroves and coral reefs during the ongoing sea-level rise not only depends on our ability to preserve the ecosystems but also on their geological preconditioning. Therefore, strategies to preserve mangrove ecosystems—while undoubtedly essential—can only be successful if accounting for their geological history.

# **Acknowledgements**

TS thanks RIIM LPDP and BRIN for the research grants in 2023, batch 3, year 2, number B-842/II.7.5/FR.06/5/2023 and B-2458/III.4/HK/5/2023. GdG acknowledges postdoctoral funding from the IRD and the Manajemen Talenta BRIN fellowship program, and research permit 52/SIP/IV/FR/6/2022 was provided by the Indonesian government on June 8, 2022. Radiocarbon dating has been carried out at the LMC14 laboratory (Saclay, France) with

financial support from the IRD to GdG. RR acknowledges the Program PDKN Nusantara Research Grant number 083/E5/PG.02.00.PT/2022. Finally, it must be noted that this research would not have been possible without the indispensable support of local authorities, including Etyn Yunita (Belitong Geopark), and our local scientific field guides Stéphane and Yadi (Go Belitung).

### **Funding Statement:**

This research was funded primarily by postdoctoral funding from the IRD and the BRIN Talent Management fellowship program to GdG (research permit 52/SIP/IV/FR/6/2022 on June 8, 2022).

#### References

- Allen Coral Atlas (2022). Imagery, maps and monitoring of the world's tropical coral reefs. https://doi.org/10.5281/zenodo.3833242
- Baharuddin & Sidarto (1995). Indonesian Geological Map. Sheet Belitung, Sumatera scale 1: 250.000. Geological Research and Development Centre.
- BIG (2024). Bathymetry of Belitung Island, Bangka Belitung. https://tanahair.indonesia.go.id/demnas/#/batnas. Accessed 26 May 2024
- Bird, M. I., Fifield, L. K., Teh, T. S., Chang, C. H., Shirlaw, N., & Lambeck, K. (2007). An inflection in the rate of early mid-Holocene eustatic sea-level rise: A new sea-level curve from Singapore. *Estuarine, Coastal and Shelf Science*, 71(3-4), 523-536. https://doi.org/10.1016/j.ecss.2006.07.004.
- Bird, M. I., Austin, W. E., Wurster, C. M., Fifield, L. K., Mojtahid, M., & Sargeant, C. (2010). Punctuated eustatic sea-level rise in the early mid-Holocene. *Geology*, *38*(9), 803-806. https://doi.org/10.1130/G31066.1.
- Buddemeier, R. W., & Smith, S. V. (1988). Coral reef growth in an era of rapidly rising sea level: predictions and suggestions for long-term research. *Coral reefs*, 7(1), 51-56. https://doi.org/10.1007/BF00301982
- Cabioch, G., Montaggioni, L. F., Faure, G., & Ribaud-Laurenti, A. (1999). Reef coralgal assemblages as recorders of paleobathymetry and sea level changes in the Indo-Pacific province. *Quaternary Science Reviews*, *18*(14), 1681-1695. https://doi.org/10.1016/S0277-3791(99)00014-1
- Cahyarini, S. Y., Pfeiffer, M., Reuning, L., Liebetrau, V., Dullo, W. C., Takayanagi, H., ... & Eisenhauer, A. (2021). Modern and sub-fossil corals suggest reduced temperature variability in the eastern pole of the Indian Ocean Dipole during the medieval climate anomaly. *Scientific reports*, 11(1), 14952. https://doi.org/10.1038/s41598-021-94465-1
- Cazenave, A., & Llovel, W. (2010). Contemporary sea level rise. *Annual review of marine science*, 2(1), 145-173. https://doi.org/10.1146/annurev-marine-120308-081105
- Choudhary, B., Dhar, V., & Pawase, A. S. (2024). Blue carbon and the role of mangroves in carbon sequestration: Its mechanisms, estimation, human impacts and conservation strategies for economic incentives. *Journal of Sea Research*, 199, 102504. https://doi.org/10.1016/j.seares.2024.102504

- Cobb, K. M., Westphal, N., Sayani, H. R., Watson, J. T., Di Lorenzo, E., Cheng, H., ... & Charles, C. D. (2013). Highly variable El Niño–southern oscillation throughout the Holocene. *Science*, *339*(6115), 67-70.
- Collins, L. B., Testa, V., Zhao, J., & Qu, D. (2011). Holocene growth history and evolution of the Scott Reef carbonate platform and coral reef. *Journal of the Royal Society of Western Australia*, 94(2), 239.
- De Gelder, G., Husson, L., Pastier, A. M., Fernández-Blanco, D., Pico, T., Chauveau, D., ... & Pedoja, K. (2022). High interstadial sea levels over the past 420ka from the Huon Peninsula, Papua New Guinea. *Communications Earth & Environment*, *3*(1), 256. https://doi.org/10.1038/s43247-022-00583-7
- De Gelder, G., Solihuddin, T., Utami, D. A., Hendrizan, M., Rachmayani, R., Chauveau, D., ... & Cahyarini, S. Y. (2023). Geodynamic control on Pleistocene coral reef development: insights from northwest Sumba Island (Indonesia). *Earth Surface Processes and Landforms*, 48(13), 2536-2553. https://doi.org/10.1002/esp.5643
- Done, T. J. (1982). Patterns in the distribution of coral communities across the central Great Barrier Reef. *Coral reefs*, 1(2), 95-107. https://doi.org/10.1007/BF00301691
- Dumoulin, J. P., Comby-Zerbino, C., Delque-Količ, E., Moreau, C., Caffy, I., Hain, S., Perron M, Thellier B, Setti V, Berthier B and Beck L. (2017). Status report on sample preparation protocols developed at the LMC14 Laboratory, Saclay, France: from sample collection to 14C AMS measurement. *Radiocarbon*, *59*(3), 713-726.
- Embry, A. F., & Klovan, J. E. (1971). A late Devonian reef tract on northeastern Banks Island, NWT. *Bulletin of Canadian petroleum geology*, *19*(4), 730-781.
- Erkan, D., & de Gelder, G. (2025). Animation coral reef mangrove evolution Belitung. figshare. Media. https://doi.org/10.6084/m9.figshare.29661044.v1
- Falter, J. L., Lowe, R. J., Zhang, Z., & McCulloch, M. (2013). Physical and biological controls on the carbonate chemistry of coral reef waters: effects of metabolism, wave forcing, sea level, and geomorphology. *PloS one*, 8(1), e53303. https://doi.org/10.1371/journal.pone.0053303
- Fernández-Blanco, D., de Gelder, G., Lacassin, R., & Armijo, R. (2019). A new crustal fault formed the modern Corinth Rift. *Earth-Science Reviews*, *199*, 102919. 10.1016/j.earscirev.2019.102919ff. ffinsu-02321883f
- Geyh, M. A., Streif, H., & Kudrass, H. R. (1979). Sea-level changes during the late Pleistocene and Holocene in the Strait of Malacca. *Nature*, *278*(5703), 441-443. https://doi.org/10.1038/278441a0
- Grossman, E. E., & Fletcher III, C. H. (2004). Holocene reef development where wave energy reduces accommodaton space, Kailua Bay, Windward Oahu, Hawaii, USA. *Journal of Sedimentary Research*, 74(1), 49-63. https://doi.org/10.1306/070203740049
- Guannel, G., Arkema, K., Ruggiero, P., & Verutes, G. (2016). The power of three: coral reefs, seagrasses and mangroves protect coastal regions and increase their resilience. *PloS one*, 11(7), e0158094. doi:10.1371/journal.pone.0158094
- Harborne, A. R., Mumby, P. J., Micheli, F., Perry, C. T., Dahlgren, C. P., Holmes, K. E., & Brumbaugh, D. R. (2006). The functional value of Caribbean coral reef, seagrass and mangrove habitats to ecosystem processes. *Advances in marine biology*, 50, 57-189. https://doi.org/10.1016/S0065-2881(05)50002-6

- Hesp, P.A., Hung, C.C., Hilton, M., Ming, C.L. and Turner, I.M. (1998). A first tentative Holocene sea-level curve for Singapore. *Journal of Coastal Research*, 14: 308-314. https://www.jstor.org/stable/4298779
- Hopley, D., Smithers, S.G., Parnell, K.E. (2007). The Geomorphology of the Great Barrier Reef. Development, Diversity, and Change. Cambridge University Press, Cambridge, pp. 546.
- Howard, J., Sutton-Grier, A., Herr, D. (2017). Clarifying the role of coastal and marine systems in climate mitigation. *Frontiers in Ecology and the Environment*, 15, 1, 42-50. <a href="https://doi.org/10.1002/fee.1451">https://doi.org/10.1002/fee.1451</a>
- Husson, L., Riel, N., Aribowo, S., Authemayou, C., de Gelder, G., Kaus, B. J. P., ... & Sarr, A. C. (2022). Slow geodynamics and fast morphotectonics in the far East Tethys. *Geochemistry, Geophysics, Geosystems*, 23(1), e2021GC010167. https://doi.org/10.1029/2021GC010167
- Hibbert, F. D., Rohling, E. J., Dutton, A., Williams, F. H., Chutcharavan, P. M., Zhao, C., & Tamisiea, M. E. (2016). Coral indicators of past sea-level change: A global repository of U-series dated benchmarks. *Quaternary Science Reviews*, *145*, 1–56. <a href="https://doi.org/10.1016/j.quascirev.2016.04.019">https://doi.org/10.1016/j.quascirev.2016.04.019</a>
- IPCC (2021). Summary For Policymakers. In: Climate Change 2021: The Physical Science Basis. Contribution of Working Group I to the Sixth Assessment Report of the Intergovernmental Panel on Climate Change. Eds. Masson-Delmotte, V., Zhai, P., Pirani, A., Connors, S.L., Péan, C., Berger, S., Caud, N., Chen, Y., et al., pp. 3-32 Cambridge, United Kingdom and New York, NY, USA: Cambridge University Press. 10.1017/9781009157896.001
- Kamila, A., Bandyopadhyay, J., & Paul, A. K. (2020). An assessment of geomorphic evolution and some erosion affected areas of Digha-Sankarpur coastal tract, West Bengal, India. *Journal of Coastal Conservation*, *24*(5), 60. https://doi.org/10.1007/s11852-020-00778-0
- Kantamaneni, K., Rice, L., Du, X., Allali, B., & Yenneti, K. (2022). Are current UK coastal defences good enough for tomorrow? An assessment of vulnerability to coastal erosion. *Coastal Management*, 50(2), 142-159. https://doi.org/10.1080/08920753.2022.2022971
- Kathiresan, K. (2021). Mangroves: types and importance. In *Mangroves: ecology, biodiversity and management* (pp. 1-31). Singapore: Springer Singapore. <a href="https://doi.org/10.1007/978-981-16-2494-0">https://doi.org/10.1007/978-981-16-2494-0</a> 1
- Khan, N. S., Ashe, E., Shaw, T. A., Vacchi, M., Walker, J., Peltier, W. R., ... & Horton, B. P. (2015). Holocene relative sea-level changes from near-, intermediate-, and far-field locations. *Current Climate Change Reports*, *1*(4), 247-262. <a href="https://doi.org/10.1007/s40641-015-0029-z">https://doi.org/10.1007/s40641-015-0029-z</a>
- Kleypas, J. A. (1996). Coral reef development under naturally turbid conditions: fringing reefs near Broad Sound, Australia. *Coral Reefs*, *15*(3), 153-167. <a href="https://doi.org/10.1007/BF01145886">https://doi.org/10.1007/BF01145886</a>
- Li, J., Knapp, D. E., Schill, S. R., Roelfsema, C., Phinn, S., Silman, M., ... & Asner, G. P. (2019). Adaptive bathymetry estimation for shallow coastal waters using Planet Dove satellites. *Remote Sensing of Environment*, 232, 111302. <a href="https://doi.org/10.1016/j.rse.2019.111302">https://doi.org/10.1016/j.rse.2019.111302</a>

- Li, T., Chua, S., Tan, F., Khan, N. S., Shaw, T. A., Majewski, J., ... & Horton, B. P. (2023). Glacial Isostatic Adjustment modelling of the mid-Holocene sea-level highstand of Singapore and Southeast Asia. *Quaternary Science Reviews*, 319, 108332. <a href="https://doi.org/10.1016/j.guascirev.2023.108332">https://doi.org/10.1016/j.guascirev.2023.108332</a>
- Malthus, T. J., & Mumby, P. J. (2003). Remote sensing of the coastal zone: an overview and priorities for future research. <a href="https://doi.org/10.1080/0143116031000066954">https://doi.org/10.1080/0143116031000066954</a>
- Mann, T., Bender, M., Lorscheid, T., Stocchi, P., Vacchi, M., Switzer, A. D., & Rovere, A. (2019). Holocene sea levels in southeast Asia, Maldives, India and Sri Lanka: the SEAMIS database. *Quaternary Science Reviews*, 219, 112-125. <a href="https://doi.org/10.1016/j.guascirev.2019.07.007">https://doi.org/10.1016/j.guascirev.2019.07.007</a>
- McGregor, H. V., Wilcox, P., Fischer, M. J., Phipps, S. J., Gagan, M. K., Wittenberg, A., ... & Chivas, A. R. (2022). Millennial to seasonal scale views of El Niño-Southern Oscillation from central Pacific corals.
- Meltzner, A. J., Switzer, A. D., Horton, B. P., Ashe, E., Qiu, Q., Hill, D. F., ... & Suwargadi, B. W. (2017). Half-metre sea-level fluctuations on centennial timescales from mid-Holocene corals of Southeast Asia. *Nature Communications*, 8(1), 14387. <a href="https://doi.org/10.1038/ncomms14387">https://doi.org/10.1038/ncomms14387</a>
- Mitchum, G. T., Nerem, R. S., Merrifield, M. A., & Gehrels, W. R. (2010). Modern sea-level-change estimates. *Understanding sea-level rise and variability*, 122-142.
- Montaggioni, L. F., & Faure, G. (1997). Response of reef coral communities to sea-level rise: a Holocene model from Mauritius (Western Indian Ocean). *Sedimentology*, *44*(6), 1053-1070. https://doi.org/10.1111/j.1365-3091.1997.tb02178.x
- Montaggioni, L. F. (2005). History of Indo-Pacific coral reef systems since the last glaciation: Development patterns and controlling factors. *Earth-Science Reviews*, 71(1), 1–75. <a href="https://doi.org/10.1016/j.earscirev.2005.01.002">https://doi.org/10.1016/j.earscirev.2005.01.002</a>
- Moreau, C., Caffy, I., Comby, C., Delqué-Količ, E., Dumoulin, J. P., Hain, S., ... & Vincent, J. (2013). Research and development of the Artemis 14C AMS Facility: status report. *Radiocarbon*, *55*(2), 331-337. doi:10.1017/S0033822200057441
- Nathan, Y., Chua, S., Chong, A., Chan, N., Morgan, K., Switzer, A. D., ... & Horton, B. P. (2025). Rapid mangrove sediment accretion in late-Holocene paleochannels of Singapore. *The Holocene*, 35(3), 259-270. <a href="https://doi.org/10.1177/09596836241297646">https://doi.org/10.1177/09596836241297646</a>
- Neal, J., Hawker, L. (2023): FABDEM V1-2. <a href="https://doi.org/10.5523/bris.s5hqmjcdj8yo2ibzi9b4ew3sn">https://doi.org/10.5523/bris.s5hqmjcdj8yo2ibzi9b4ew3sn</a>. Accessed 15 March 2024
- Neumann, A. C. (1985). Reef response to sea level rise: Keep-up, catch-up or give-up. In *Proc. Fifth Intern. Coral Reef Congr. Tahiti* (Vol. 3, pp. 105-110).
- Pamungkas, A. (2018). Karakteristik parameter oseanografi (pasang-surut, arus, dan gelombang) di perairan utara dan selatan Pulau Bangka. *Buletin Oseanografi Marina*, 7(1), 51-58. <a href="https://doi.org/10.14710/buloma.v7i1.19042">https://doi.org/10.14710/buloma.v7i1.19042</a> (in Indonesia)
- Priem, H. N. A., Boelrijk, N. A. I. M., Hebeda, E. H., Verdurmen, E. A., Verschure, R. H., & Bon, E. H. (1975). Isotope geochronology in the Indonesian tin belt. Geol. en Mijnb, vol 54 (1), p.61-70
- Rahmstorf S. (2007). A semi-empirical approach to projecting future sea level rise. *Science* 315:368

- Ramsey, C. B. (2009). Bayesian analysis of radiocarbon dates. *Radiocarbon*, 51(1), 337-360. <a href="https://c14.arch.ox.ac.uk/oxcal/OxCal.html#">https://c14.arch.ox.ac.uk/oxcal/OxCal.html#</a>. Accessed 12 October 2023
- Rogers, A., & Mumby, P. J. (2019). Mangroves reduce the vulnerability of coral reef fisheries to habitat degradation. *PLoS biology*, *17*(11), e3000510. <a href="https://doi.org/10.1371/journal.pbio.3000510">https://doi.org/10.1371/journal.pbio.3000510</a>
- Saintilan, N., Khan, N. S., Ashe, E., Kelleway, J. J., Rogers, K., Woodroffe, C. D., & Horton, B. P. (2020). Thresholds of mangrove survival under rapid sea level rise. *Science*, 368(6495), 1118-1121. DOI: 10.1126/science.aba2656
- Saintilan, N., Horton, B., Törnqvist, T. E., Ashe, E. L., Khan, N. S., Schuerch, M., ... & Guntenspergen, G. (2023). Widespread retreat of coastal habitat is likely at warming levels above 1.5 C. *Nature*, *621*(7977), 112-119. <a href="https://doi.org/10.1038/s41586-023-06448-z">https://doi.org/10.1038/s41586-023-06448-z</a>
- Sarr, A. C., Husson, L., Sepulchre, P., Pastier, A.-M., Pedoja, K., Elliot, M., Arias-Ruiz, C., Solihuddin, T., Aribowo, S., & Susilohadi. (2019). Subsiding Sundaland. *Geology*, 47(2), 119–122. https://doi.org/10.1130/G45629.1
- Scheffers, A., Brill, D., Kelletat, D., Brückner, H., Scheffers, S., & Fox, K. (2012). Holocene sea levels along the Andaman Sea coast of Thailand. *The Holocene*, *22*(10), 1169-1180. <a href="https://doi.org/10.1177/0959683612441803">https://doi.org/10.1177/0959683612441803</a>.
- Scoffin, T. P., & Tissier, M. L. (1998). Late Holocene Sea level and reef-flat progradation, Phuket, South Thailand. *Coral Reefs*, 17(3), 273-276. https://doi.org/ 10.1007/s003380050128.
- Shaw, T. A., Li, T., Ng, T., Cahill, N., Chua, S., Majewski, J. M., ... & Horton, B. P. (2023). Deglacial perspectives of future sea level for Singapore. *Communications Earth & Environment*, *4*(1), 204. <a href="https://doi.org/10.1038/s43247-023-00868-5">https://doi.org/10.1038/s43247-023-00868-5</a>
- Short, A. D. (2012) Coastal Processes and Beaches. Nature Education Knowledge 3(10):15.
- Solihuddin, T., Collins, L. B., Blakeway, D., & O'Leary, M. J. (2015). Holocene coral reef growth and sea level in a macrotidal, high turbidity setting: Cockatoo Island, Kimberley Bioregion, northwest Australia. *Marine Geology*, 359, 50-60. <a href="http://dx.doi.org/10.1016/j.margeo.2014.11.011">http://dx.doi.org/10.1016/j.margeo.2014.11.011</a>
- Solihuddin, T., O'Leary, M. J., Blakeway, D., Parnum, I., Kordi, M., & Collins, L. B. (2016). Holocene reef evolution in a macrotidal setting: buccaneer archipelago, kimberley bioregion, northwest Australia. *Coral Reefs*, *35*(3), 783-794. doi:10.1007/s00338-016-1424-1
- Solihuddin, T., Bufarale, G., Blakeway, D., & O'Leary, M. J. (2016). Geomorphology and late Holocene accretion history of Adele Reef: a northwest Australian mid-shelf platform reef. *Geo-Marine Letters*, *36*(6), 465-477. <a href="http://dx.doi.org/10.1007/s00367-016-0465-3">http://dx.doi.org/10.1007/s00367-016-0465-3</a>.
- Srivastava, J., & Prasad, V. (2019). Evolution and paleobiogeography of mangroves. *Marine Ecology*, 40(6), e12571. DOI: 10.1111/maec.12571
- Sui, C., de Vos, P., Stapersma, D., Visser, K., & Ding, Y. (2020). Fuel consumption and emissions of ocean-going cargo ship with hybrid propulsion and different fuels over voyage. *Journal of marine science and engineering*, 8(8), 588. <a href="https://doi.org/10.3390/jmse8080588">https://doi.org/10.3390/jmse8080588</a>

- Susanto, R. D., Gordon, A. L., & Zheng, Q. (2001). Upwelling along the coasts of Java and Sumatra and its relation to ENSO. *Geophysical Research Letters*, 28(8), 1599-1602. https://doi.org/10.1029/2000GL011844
- Susilohadi, S., Novico, F., Husson, L., Rahardiawan, R., Prabowo, H., Widodo, J., & Sudjono, E. H. (2024). Quaternary deposition and erosion in the northeastern Sunda Strait: An interplay between sea level, tectonics, and magmatic activity. *Journal of Asian Earth Sciences: X*, 12, 100179. <a href="https://doi.org/10.1016/j.jaesx.2024.100179">https://doi.org/10.1016/j.jaesx.2024.100179</a>
- Suyarso, S. (2012). Melacak Perubahan Muka Laut Masa Lampau Berdasar Fosil Kerangkerangan (Ostrea sp.) di Pulau Belitung. *ILMU KELAUTAN: Indonesian Journal of Marine Sciences*, 15 (3), 135-142 (doi:10.14710/ik.ijms.15.3.135-142)
- Takahashi, T. (1988). Relationship between reef growth and sea level on the northwest coast of Kume Island, the Ryukyus: Date from drill holes on the Holocene coral reef. In *Proceedings of the sixth international coral reef symposium, Townsville, Australia 8th-12th August 1988 volume 3: Contributed pap* (pp. 491-496). The 6th International Coral Reef Symposium Executive Committee.
- Tanabe, S., Hori, K., Saito, Y., Haruyama, S., Vu, V. P., & Kitamura, A. (2003). Song Hong (Red River) delta evolution related to millennium-scale Holocene sea-level changes. *Quaternary Science Reviews*, 22(21-22), 2345-2361. doi:10.1016/S0277-3791(03)00138-0
- Thom, B. G., Wright, L. D., & Coleman, J. M. (1975). Mangrove ecology and deltaicestuarine geomorphology: Cambridge Gulf-ord river, western Australia. *The Journal of Ecology*, 203-232. <a href="https://doi.org/10.2307/2258851">https://doi.org/10.2307/2258851</a>
- Tjia, H. D. (1996). Sea-level changes in the tectonically stable Malay-Thai Peninsula. Quaternary International, 31, 95-101. <a href="https://doi.org/10.1016/1040-6182(95)00025-E">https://doi.org/10.1016/1040-6182(95)00025-E</a>
- Tjia, H. D., & Liew, K. K. (1996). Changes in tectonic stress field in northern Sunda Shelf basins. *Geological Society, London, Special Publications*, 106(1), 291-306. <a href="https://doi.org/10.1144/GSL.SP.1996.106.01.19">https://doi.org/10.1144/GSL.SP.1996.106.01.19</a>
- Xu, T. F., Wei, Z. X., Susanto, R. D., Li, S. J., Wang, Y. G., Wang, Y., et al. (2021). Observed water exchange between the South China Sea and Java Sea through Karimata Strait. *Journal of Geophysical Research: Oceans*, 126, e2020JC016608. <a href="https://doi.org/10.1029/2020JC016608">https://doi.org/10.1029/2020JC016608</a>
- van Woesik, R., & Done, T. J. (1997). Coral communities and reef growth in the southern Great Barrier Reef. *Coral Reefs*, 16(2), 103-115. <a href="https://doi.org/10.1007/s003380050064">https://doi.org/10.1007/s003380050064</a>
- Veron, J. E. N. (2000). Corals of the World. Australian Inst. Mar. Sci., vol. 3, 463 pp.+429 pp. +490 pp.
- Vitousek, S., Buscombe, D., Vos, K., Barnard, P. L., Ritchie, A. C., & Warrick, J. A. (2023). The future of coastal monitoring through satellite remote sensing. *Cambridge Prisms: Coastal Futures*, 1, e10. https://doi.org/10.1017/cft.2022.4
- Wells, S., & Ravilious, C. (2006). *In the front line: shoreline protection and other ecosystem services from mangroves and coral reefs* (No. 24). UNEP/Earthprint.
- Whitfield, A. K. (2017). The role of seagrass meadows, mangrove forests, salt marshes and reed beds as nursery areas and food sources for fishes in estuaries. *Reviews in*

- Fish Biology and Fisheries, 27(1), 75-110. <u>https://doi.org/10.1007/s11160-016-9454-</u>x
- Woodroffe, C. D., Thom, B. G., & Chappell, J. (1985). Development of widespread mangrove swamps in mid-Holocene times in northern Australia. *Nature*, *317*(6039), 711-713. <a href="https://doi.org/10.1038/317711a0">https://doi.org/10.1038/317711a0</a>
- Woodroffe, C. (1992). Mangrove sediments and geomorphology. *Tropical mangrove* ecosystems, 41, 7-41. DOI:10.1029/CE041
- Woodroffe, C. D. (2002). Coasts: form, process and evolution. Cambridge University Press.
- Woodroffe, S. A., & Horton, B. P. (2005). Holocene sea-level changes in the Indo-Pacific. *Journal of Asian earth sciences*, 25(1), 29-43. <a href="https://doi.org/10.1016/j.jiseaes.2004.01.009">https://doi.org/10.1016/j.jiseaes.2004.01.009</a>
- Woodroffe, C. D., Rogers, K., McKee, K. L., Lovelock, C. E., Mendelssohn, I. A., & Saintilan, N. (2016). Mangrove sedimentation and response to relative sea-level rise. *Annual review of marine science*, *8*, 243-266. 10.1146/annurev-marine-122414-034025
- Woodroffe, C. D. (2025). Biogeomorphological inheritance: The legacy of past landforms constrains future tropical coastal landscapes. *Earth Surface Processes and Landforms*, 50(2), e70013. https://doi.org/10.1002/esp.70013
- Worthington, T. A., Zu Ermgassen, P. S., Friess, D. A., Krauss, K. W., Lovelock, C. E., Thorley, J., ... & Spalding, M. (2020). A global biophysical typology of mangroves and its relevance for ecosystem structure and deforestation. *Scientific reports*, *10*(1), 14652. <a href="https://doi.org/10.1038/s41598-020-71194-5">https://doi.org/10.1038/s41598-020-71194-5</a>
- Wyrtki, K. (1961). *Physical oceanography of the Southeast Asian waters* (Vol. 2). University of California, Scripps Institution of Oceanography.
- Yamano, H., Hori, K., Yamauchi, M., Yamagawa, O., & Ohmura, A. (2001). Highest-latitude coral reef at Iki Island, Japan. *Coral Reefs*, 20(1), 9-12. DOI: 10.1007/s003380100137
- Yamano, H., Inoue, T., Adachi, H., Tsukaya, K., Adachi, R., & Baba, S. (2019). Holocene sea-level change and evolution of a mixed coral reef and mangrove system at Iriomote Island, southwest Japan. *Estuarine, Coastal and Shelf Science*, 220, 166-175. <a href="https://doi.org/10.1016/j.ecss.2019.03.001">https://doi.org/10.1016/j.ecss.2019.03.001</a>
- Yulianto, E., Rahardjo, A.T., Noeradi, D., Siregar, D.A., Hirakawa, K. (2005). A Holocene pollen record of vegetation and coastal environmental changes in the coastal swamp forest at Batulicin, South Kalimantan, Indonesia. Journal of Asian Earth Sciences, 25(1), 1–8. doi:10.1016/j.iseaes.2004.01.005
- Yulianto, E., Sukapti, W. S., & Praptisih, P. (2019). Perubahan Lingkungan dan Evolusi Mangrove di Pulau Belitung Selama Holosen Akhir Berdasarkan Rekaman Polen. *Jurnal Geologi Kelautan*, *17*(2). <a href="http://dx.doi.org/10.32693/jgk.17.2.2019.578">http://dx.doi.org/10.32693/jgk.17.2.2019.578</a> (in Indonesia)